

Analysis of exchange interactions in dimers of Mn_3 single-molecule magnets, and their sensitivity to external pressure

Jie-Xiang Yu^{1,2,3}, George Christou^{2,4} and Hai-Ping Cheng^{1,2,4*}

¹Department of Physics, ²The M²QM Center, ³The Quantum Theory Project and

⁴Department of Chemistry

Abstract

In light of the potential use of single-molecule magnets (SMMs) in emerging quantum information science initiatives, we report first-principles calculations of the magnetic exchange interactions in $[Mn_3]_2$ dimers of Mn_3 SMMs, connected by covalently-attached organic linkers, that have been synthesized and studied experimentally by magnetochemistry and EPR spectroscopy. Energy evaluations calibrated to experimental results give the sign and order of magnitude of the exchange coupling constant (J_{12}) between the two Mn_3 units that match with fits of magnetic susceptibility data and EPR spectra. Downfolding into the Mn d -orbital basis, Wannier function analysis has shown that magnetic interactions can be channeled by ligand groups that are bonded by van der Waals interaction and/or by the linkers via covalent bonding of specific systems, and effective tight-binding Hamiltonians are obtained. We call this long-range coupling that involves a group of atoms a *collective exchange*. Orbital projected spin density of states and alternative Wannier transformations support this observation. To assess the sensitivity of J_{12} to external pressure, stress-strain curves have been investigated for both hydrostatic and uniaxial pressure, which have revealed a switch of J_{12} from ferromagnetic to antiferromagnetic with increasing pressure.

Magnetic molecules have stimulated intense interest in chemistry and physics because of their potential applications in quantum information science ¹⁻⁴ and other future technologies ⁵⁻⁸. One important class of magnetic molecules are single-molecule magnets (SMMs), which have a sufficiently large anisotropy barrier vs kT to magnetization relaxation that they behave as nanoscale magnets. One of the most investigated properties in SMMs is quantum tunneling of the magnetization vector (QTM) through the anisotropy barrier⁹⁻¹³. In dimers of Mn_4 SMMs with $S = 9/2$ held together by hydrogen-bonding, the resulting weak inter- Mn_4 exchange coupling led to discovery of new phenomena in molecular magnetism, namely (i) exchange-biased QTM whereby the neighboring Mn_4 acted as a bias field shifting the position of the QTM steps in the hysteresis loop¹¹, and (ii) the generation of quantum superposition and entanglement states of the two Mn_4 units, which were identified by analysis of the high-frequency EPR (HF-EPR) spectra¹². More recently in 2007, triangular $[Mn_3O(O_2CR)_6(py)_3](ClO_4)$ SMMs (R = Me, Et, Ph) were synthesized containing three ferromagnetically-coupled Mn^{III} ions and an $S = 6$ ground state ¹⁴. Covalent linkage of these Mn_3 SMMs with organic linkers provides a more controlled method than hydrogen-bonding to synthesize a variety of $[Mn_3]_2$ dimers¹⁴ and higher $[Mn_3]_4$ oligomers¹⁰. The covalent linkage introduces weak exchange coupling between two Mn_3 units in dimers or tetramers,

and its sign can be varied depending on the linker identity. These dimers and tetramers were obtained as molecular crystals permitting full structural characterization by X-ray crystallographic studies.

The primary subject of this paper is the $[\text{Mn}_3]_2$ dimer with dpd^{2-} linkers (dpd^{2-} = the dianion of 1,3-di(pyridin-2-yl)propane-1,3-dione dioxime), which was found by magnetic susceptibility measurements and HF-EPR spectroscopy to have a ferromagnetic (**FM**) interaction (J_{12}) between the two Mn_3 units ¹⁴. In addition, HF-EPR was employed to investigate the resulting quantum superposition states in both the crystal and solution phases ¹⁴. The spin Hamiltonian employed was $\hat{H} = \hat{H}_1 + \hat{H}_2 - 2J_{12}\hat{S}_1 \cdot \hat{S}_2$ with $\hat{H}_{1,2} = D\hat{S}_{1,2z}^2 + g\mu_B\hat{S} \cdot \vec{H}$, where $\hat{S}_{1,2}$ and $\hat{H}_{1,2}$ are the spin and the spin Hamiltonian of each Mn_3 unit 1 and 2, \hat{S}_z is the spin projection along the easy axis, the anisotropy $D = -0.22 \text{ cm}^{-1}$, and $g_z = 2.00$; μ_B is the Bohr magneton and μ_0 is the vacuum permeability. Both the fits of magnetic and EPR data give $J_{12} = 0.025 \text{ cm}^{-1}$.

In the absence of theoretical calculations, it was proposed ¹⁵ that the Mn d_π magnetic orbitals delocalize into the $\text{dpd}^{2-} \pi$ systems and the J_{12} exchange coupling is propagated by spin polarization of the bonding electrons in the central sp^3 C atom of the linker. Does this explanation give the exact microscopic physics of magnetic exchange in the $[\text{Mn}_3]$ dimer? This is the first question we decided to address. The second question is if and how one can tune the J_{12} interaction of a given dimer, and thus the resulting quantum properties. This requires an assessment of the sensitivity of J_{12} to external influences, and an experimentally feasible method is to apply external pressure and see how coupling strength changes. Pressure-dependent investigations have lately become extensively used to uncover new physics behaviors in various materials and states of matter. Particular to magnetic orderings, pressure-dependent structural changes lead to changes in charge and spin ordering, magnetic properties, superconducting transitions ¹⁶⁻¹⁷ and transport behavior in perovskites ¹⁸⁻²¹. Specific to molecular magnetic materials, pressure- or strain-dependent studies include enhancing the magnetic ordering temperature in rhenium(IV) molecules ²², changing steps in quantum tunneling magnetization ²³, and modulating tunneling splitting ²⁴. It is worthwhile to mention that sometimes ‘chemical pressure’ (ligand-induced perturbation of magnetic cores) is used to modulate magnetic ordering in molecular magnetic systems via altering the volume of solid unit cells ²⁵⁻²⁶.

In this letter, we report results from first-principles calculations within the framework of density functional theory ²⁷⁻²⁸. We will show below that our investigations provide electronic and magnetic structures that are necessary for understanding long-range *collective magnetic exchange* interaction, test the validity of isolated ions model vs. full-crystal models, and provide strain-stress-magnetism relations. Answers to the two questions posted above will fill gaps in current knowledge of SMM clusters and in theoretical modelling, and guide future experiments and the design of new electronic magnetic materials that are pivotal for next generation electronics and technology for quantum information sciences.

Our DFT-based calculations are performed with projector augmented wave pseudopotentials²⁹ implemented in the Vienna ab initio simulation³⁰ (VASP) package. The generalized gradient approximation (GGA) in Perdew, Burke, and Ernzerhof (PBE) formation²⁸ is used as the exchange-correlation energy and the Hubbard U method³¹⁻³² ($U=2.8$ eV, $J=0.9$ eV) is applied on Mn(3d) orbitals to include strong-correlation effects. The magnitude of U is determined by the experimental result for the energy difference between inter-[Mn₃] FM and AFM spin configurations per dimer $E_{AF} - E_{FM}$ of about 0.2 meV [see Supplementary Material for details]. An energy cutoff of 600 eV is used for the plane-wave expansion throughout the calculations. The DFT-D3 method with inclusion of van der Waals correction³³ is employed. Total energy, structure optimizing, and electronic structure calculations were performed on three single-molecule [Mn₃]-dimers and their ions (we call these gas phase molecules or ions) and one FM dimer in its bulk form. For ions with charge in gas phases, the jellium model is used to keep the whole system charge neutral, and a periodic cubic lattice with lattice constant 24.00~30.00 Å is used to keep molecules sufficiently separated in adjacent unit cells. The Γ point only is used for both gas and bulk phases. A $3 \times 3 \times 3$ Γ -centered \mathbf{k} -mesh for bulk phases is used for the density-of-state (DOS) calculations. During most structure optimizing calculations, all forces on each atom are less than 1 meV/Å, or 0.2 meV/Å when external strain is applied. With these criteria, the error of the total energy difference between ferromagnetic (FM) and antiferromagnetic (AFM) spin configurations $\delta(E_{AF} - E_{FM})$ is estimated to be about 0.05 meV, which might be reduced further with an energy cutoff larger than 600 eV. After we obtain the eigenstates and eigenvalues, a unitary transformation of Bloch waves is performed to construct the tight-binding Hamiltonian in a Wannier function (WF) basis by using the maximally localized Wannier functions (MLWF) method³⁴ implemented in the Wannier90 package³⁵. The WF-based Hamiltonian has the same exact eigenvalues as those obtained by DFT calculations within an inner energy window, and the outer energy window used for downfolding WF basis is that for all the DFT Bloch states.

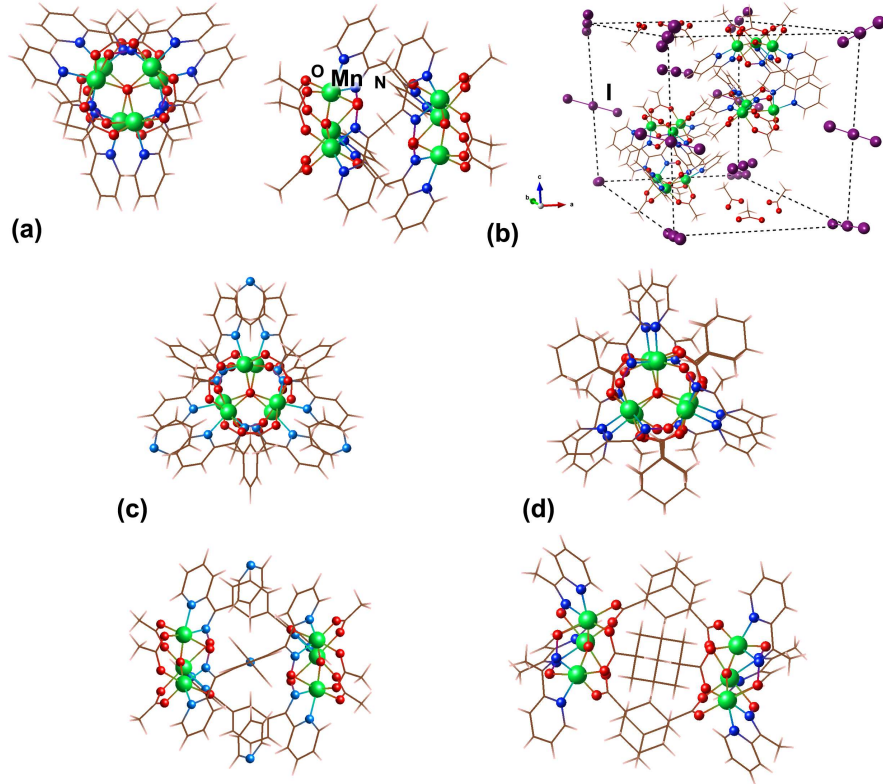


Fig. 1 structure of $([Mn_3]_2\text{-}(dpd)_3)^{2+}$, in (a) gas phase and (b) crystal phase. Structure of a (c) $([Mn_3]_2\text{-}(ppmd)_3)^{2+}$ and (d) $([Mn_3]_2\text{-}(ada)_3)^{2+}$ molecule.

The structures of three SMM $[Mn_3]_2$ dimers are shown in Fig. 1, where two $Mn_3O(O_2CMe)_3$ units are linked covalently by three different linkers. Each $[Mn_3]$ unit has C_3 symmetry and a $S = 6$ spin ground state from FM coupling of its three Mn^{3+} ions (each $S = 2$). In the resulting dimer, the two Mn_3 triangular planes made are parallel. The dimer with the shortest linker is $([Mn_3]_2\text{-}(dpd)_3)^{2+}$. For this system we investigated its crystalline phase as well as individual dimers in isolation. According to experiment ¹⁵, the molecular crystal phase of the $([Mn_3]_2\text{-}(dpd)_3)^{2+}$ dimer has space group $P\bar{3} 1c$ with trigonal symmetry in the hexagonal lattice. Each unit cell contains two dimers, which are parallel. The counterions of the $([Mn_3]_2\text{-}(dpd)_3)^{2+}$ dimer are two I_3^- anion, so that each unit cell contains four I_3^- . Structure optimization was performed with experimental lattice constants $a = 16.569 \text{ \AA}$, $c = 18.285 \text{ \AA}$; Figure 1b shows the optimized atomic structure of $([Mn_3]_2\text{-}(dpd)_3)^{2+}$.

$(dpd)_3)_2(I_3)_4$, even though experimental studies could not determine the location and orientation of the I_3^- counter ions.

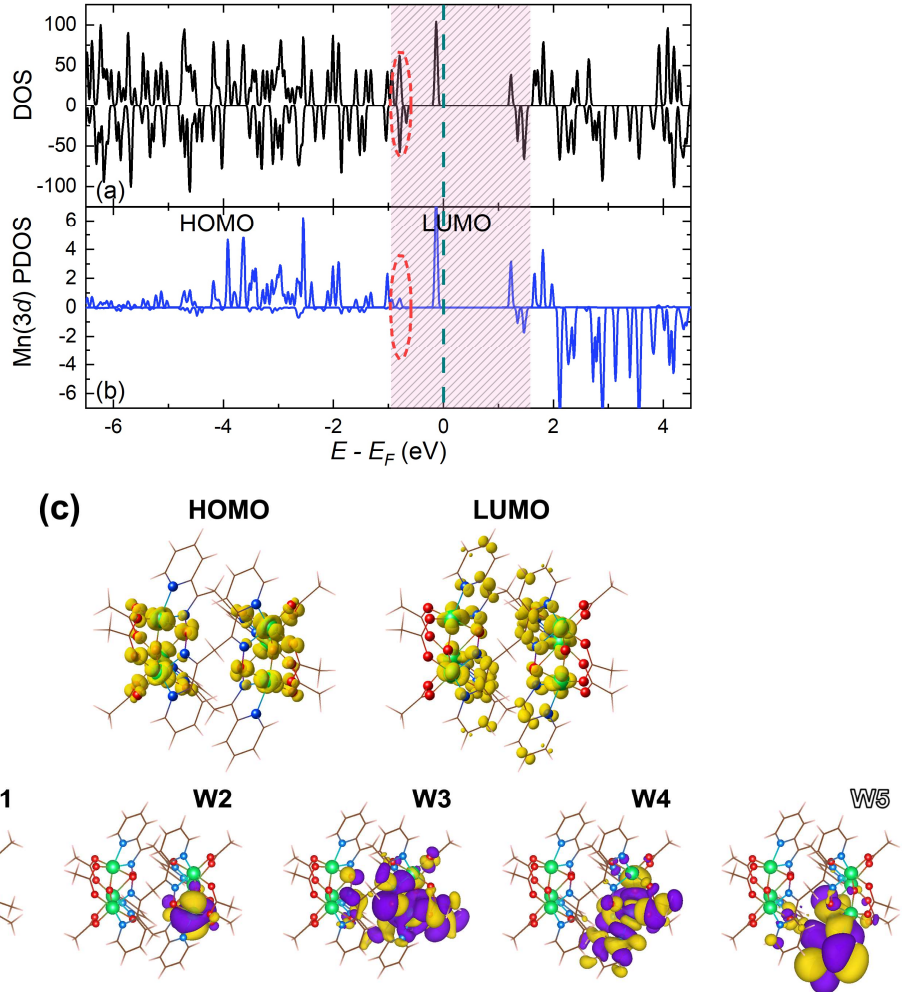


Fig. 2 Electronic structure for the gas phase of $([Mn_3]_2-(dpd)_3)^{2+}$ dimers. (a) The total density-of-state (DOS) and (b) orbit-resolved projected DOS (PDOS) of Mn(3d) orbitals. Positive and negative values correspond to spin-majority and spin-minority channels respectively. The Fermi level is set to zero. The marked state refers to the sub-HOMO state with few Mn(3d) components and the shadow region refers to the inner energy window for MLWF. (c) Partial charge density of HOMO (left) and LUMO (right). (d) Aligned by on-site energies, five Wannier functions (WFs) in the spin-majority channel centered on the same Mn atom. Solid and hollow labels represent occupied and unoccupied WFs respectively.

The calculated ground state of the isolated (gas phase) $([Mn_3]_2-(dpd)_3)^{2+}$ dimer has spin equal to 12, with each $[Mn_3]$ monomer in a $S = 6$ spin state (magnetic moment = $12\mu_B$). Fig. 2a-b shows the total DOS and projected density-of-state (PDOS) of Mn(3d) orbitals. The gap between the

highest occupied molecular orbital (HOMO) and the lowest unoccupied molecular orbital (LUMO) is 1.2 eV. The isosurfaces of HOMO and LUMO partial charge density shown in Fig. 2c are all in the spin-majority or spin-up channel, and both are dominated by Mn(3d) orbitals. However, just below the HOMO, the states circled by red dashed lines (Fig. 2a&b) have few features of Mn(3d).

The inter-Mn₃ magnetic interaction is weak but long-range. It is best not described as superexchange, which usually involves a single bridging or a few atoms. We therefore denote the magnetic exchange that involves at least one group of atoms as *collective exchange*. To understand the states near the HOMO and LUMO and how they affect the inter-Mn₃ exchange interaction, we performed MLWF calculations to get the WF-based Hamiltonian using the inner energy window shown in Fig. 2a&b, with Mn(3d) orbitals as the initial projections of Wannier functions for the downfolding process. Fig. 2d shows the five WFs in the spin-majority channel with basis function concentrated on one Mn atom. The two WFs, W1 and W2, with lowest on-site energies about -3.0 eV relative to the Fermi level in the DOS, are just localized on Mn. Three other WFs, W3 to W5 with higher on-site energies, however, have significant contribution from the ligand O₂CMe, indicating that the sub-HOMO states are dominated by ligand orbitals. More discussion about ligands is included in the supplementary materials. Considering the $S = 2$ spin state of Mn with four unpaired 3d electrons, W5 with the highest on-site energy is the only unoccupied WF in this WF basis. Other WFs centered on other Mn atoms have similar behaviors, so that W1 to W5 can be regarded as five groups to classify the thirty total WFs in the Hamiltonian. The strongest hopping t in the Hamiltonian between WFs belonging to different sides of the dimer is about 0.070 eV. It comes from one W3-like occupied WF at one side of the dimer and one W5-like unoccupied WF at the other side. Note that the overlap between W3 and W5 is dominated by two acetate ligands (one from each Mn₃ unit) instead of linkers and the energy level for the dpd linker is far below HOMO (See Fig.S1a in Supplementary materials). Because the distance between two acetate ligands of different sides is 2.53 Å which is in the region of van der Waals interaction, the exchange interaction in this system has major contribution from van der Waals bonded acetate ligands instead of covalent linkers. Magnetic coupling between two van der Waals layers is a subject of great current interest ³⁶. The electronic structure of the bulk phase ([Mn₃]₂-(dpd)₃)₂(I₃)₄ has also been investigated. The FM spin configuration shows that the total spin in one unit cell is $S = 24$ with magnetic moment $48 \mu_B$, so that each [Mn₃] monomer still has a $S = 6$ spin state with magnetic moment $12.0 \mu_B$, indicating the same valence state of the ([Mn₃]₂-(dpd)₃)²⁺ cation as that in the gas phase.

For the other two [Mn₃] dimers, experiments found that ([Mn₃]₂-(ada)₃)²⁺ has a AFM coupling between two [Mn₃] monomers, while the inter-monomer coupling in ([Mn₃]₂-(ppmd)₃)²⁺ is FM. Our total energy calculations for both of them show that $E_{AF} - E_{FM}$ for ([Mn₃]₂-(ada)₃)²⁺ is -0.02 meV per dimer and that for ([Mn₃]₂-(ppmd)₃)²⁺ is 0.03 meV per dimer. These results for $|E_{AF} - E_{FM}|$ are one order smaller than that for ([Mn₃]₂-(dpd)₃)²⁺ and are within our numerical

error. However, we can still obtain insight into electronic structure and exchange pathways. The

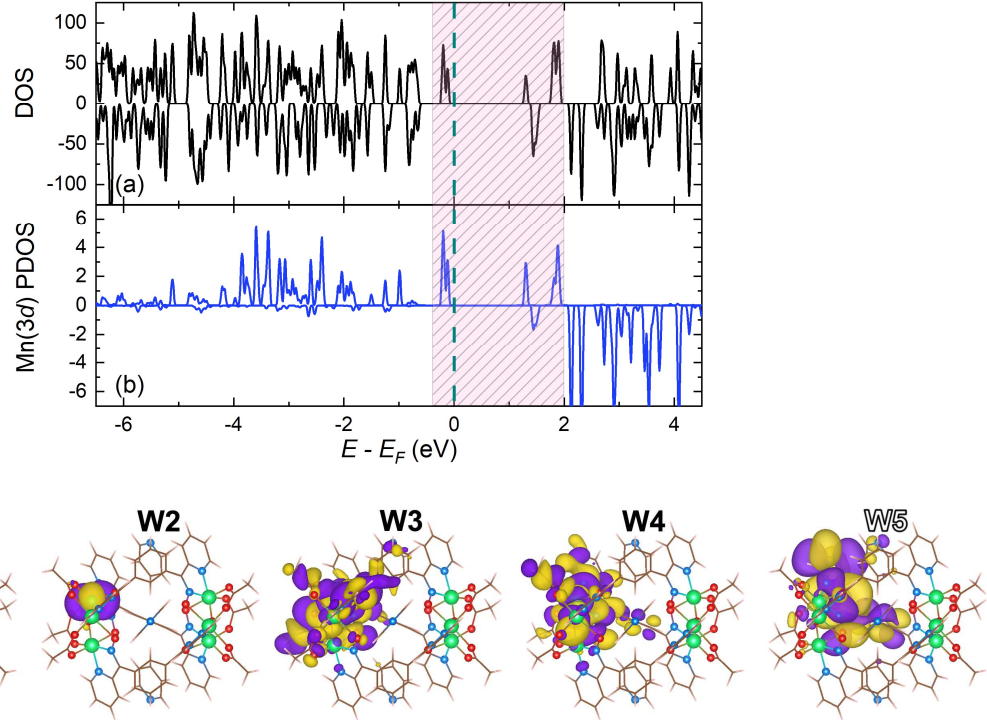


Fig. 3 Electronic structure for the gas phase of $([Mn_3]_2\text{-}(ppmd)_3)^{2+}$ dimers. (a) The total DOS and (b) PDOS of Mn(3d) orbitals. The shadow region refers to the inner energy window for MLWF. (c) Ordered by on-site energies, five WFs in the spin-majority channel centered on the same Mn atom. Solid/hollow labels represent occupied and unoccupied WFs respectively.

tiny inter-Mn₃ exchange can be explained by the electronic structure. Fig. 3a-b shows the total DOS and PDOS of Mn(3d) orbitals for $([Mn_3]_2\text{-}(ppmd)_3)^{2+}$ dimers. The DOS and PDOS are very similar to that for $([Mn_3]_2\text{-}(dpd)_3)^{2+}$, where the HOMO and LUMO are dominated by Mn(3d) orbitals and the sub-HOMOs do not have features of Mn(3d). The atomic-centered WFs for the tight-binding Hamiltonian for $([Mn_3]_2\text{-}(ppmd)_3)^{2+}$ [Fig. 3c] are also similar to those in $([Mn_3]_2\text{-}(dpd)_3)^{2+}$, where two localized WFs have lower on-site energies, and three other WFs with higher on-site energies have some features of the acetate ligand O₂CMe but mostly the linker ppmd, indicating that the linkers are responsible for the exchange couplings. In the WF basis for $([Mn_3]_2\text{-}(ppmd)_3)^{2+}$, W5 with the highest on-site energy is unoccupied. Among all the inter-Mn₃ hopping in the Hamiltonian, the strongest hopping t between occupied and unoccupied WFs is -0.016 eV, which again comes from the hopping between the occupied W3-like WF and the unoccupied W5-like WF. Thus, $([Mn_3]_2\text{-}(ppmd)_3)^{2+}$ has much weaker inter-Mn₃ hopping. Linker ppmd with a larger

size than dpd makes both the hopping crossing the linker and the exchange through the van der

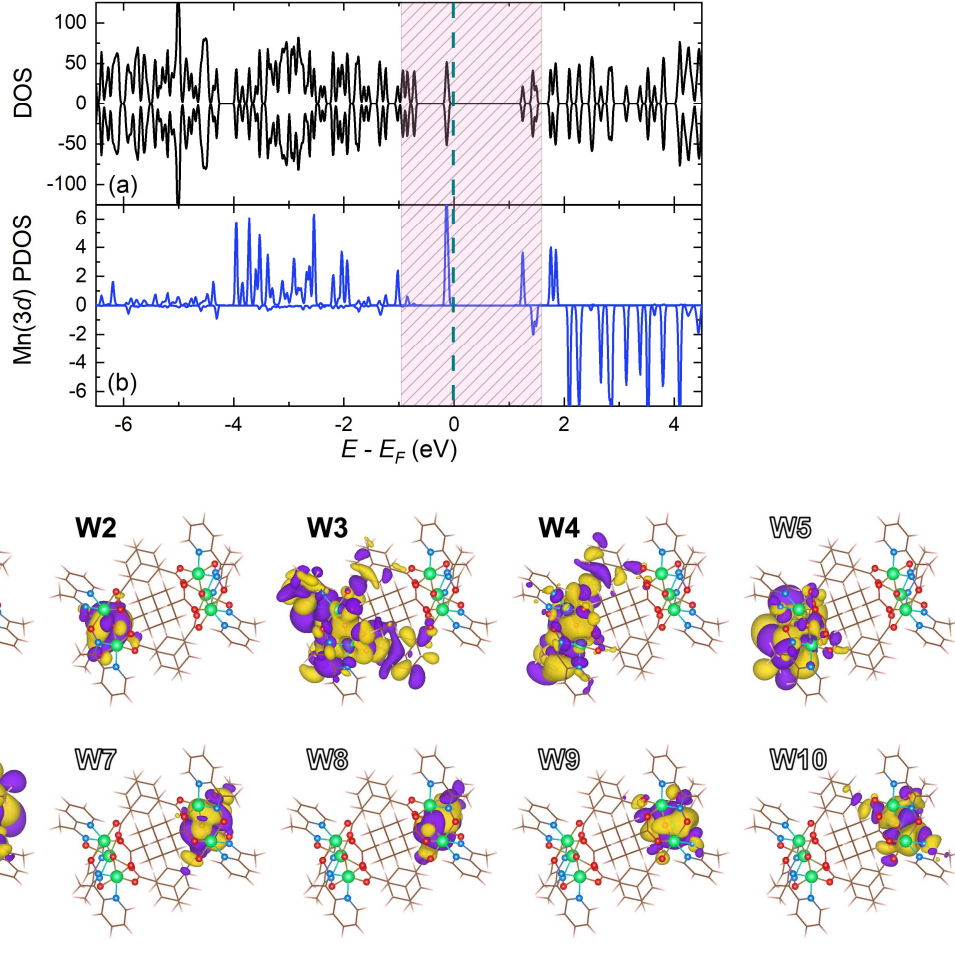


Fig. 4 Electronic structure for the gas phase of $([Mn_3]_2\text{-}(ada)_3)^{2+}$ dimers with AFM spin ordering. (a) The total DOS and (b) PDOS of Mn(3d) orbitals. The shadow region refers to the inner energy window for MLWF. (c) In the spin-majority channel, ten WFs, of which five are centered on an Mn atom at one side of the dimer and the other five centered on the corresponding Mn atom at the other side. These WFs are ordered by on-site energies, and solid/hollow labels represent occupied/unoccupied WFs respectively.

Waals bonded ligands weak. Numerically, the strength of the exchange interaction, which is usually proportional to t^2 for $([Mn_3]_2\text{-}(ppmd)_3)^{2+}$ is about one order smaller than that for $([Mn_3]_2\text{-}(dpd)_3)^{2+}$, consistent with the total energy results.

The DOS results for AFM $([Mn_3]_2\text{-}(ada)_3)^{2+}$ are shown in Fig. 4a&b. Due to AFM spin-ordering, the total DOS are identical in both spin channels. The PDOS on one Mn still gives the $S = 2$ high-spin state, the same with that for the other two dimers. The atomic-centered WFs for the tight-binding Hamiltonian are also obtained. Note that for this dimer, the two Mn_3 units are bonded only

through covalent linkers. In the same spin channel, Fig. 4c gives ten WFs, with five of them, W1 to W5, centered on a Mn atom at one side of the dimer and the other five, W6 to W10, centered on the corresponding Mn atom at the other side. That means W1 to W5 are the spin-up atomic-like orbitals of one Mn and W6 to W10 are the spin-down atomic-like orbitals of another. Because of $S = 2$ high-spin state of Mn with four unpaired $3d$ electrons, the four WFs, W1 to W4, with the lowest energies are occupied in this tight-binding basis and others are unoccupied. Among the occupied WFs, W1 and W2 are localized on Mn while W3 and W4 has a comparatively significant contribution from the ada linkers. Among the unoccupied WFs at the other side of the dimer, all WFs except for W6 are localized on Mn. The strongest inter-monomer hopping t in the Hamiltonian between occupied and unoccupied WFs are -0.015 eV between W3 and W10. The value of t^2 is only one twentieth of that in $([Mn_3]_2-(dpd)_3)^{2+}$. Considering that the only difference between $([Mn_3]_2-(dpd)_3)^{2+}$ and $([Mn_3]_2-(ada)_3)^{2+}$ is the different linkers, which affect the strength of inter-Mn₃ hopping, we can estimate that the strength of the exchange interaction of $([Mn_3]_2-(ada)_3)^{2+}$ is one twentieth in magnitude of that in $([Mn_3]_2-(dpd)_3)^{2+}$, numerically consistent with the total energy results.

Although HF-EPR experiments ¹⁵ have shown that covalently-linked [Mn₃]₂ dimers remain intact in the solution phase and retain their J12 exchange coupling and resulting quantum superposition states, their low Young's modulus in the solid phase suggests a non-trivial strain-sensitive response. To study the strain response of the J12 magnetic interaction, we applied external strain on $([Mn_3]_2-(dpd)_3)_2(I_3)_4$ by changing the lattice constant. Fig. 5a&b shows the isotropic strain-dependent results. The value of $E_{AF} - E_{FM}$ as a function of strain shows that the magnetic interaction can transition from FM to AFM when a compressive strain of about 0.4% in length, or 1.2% in volume, is applied. The hydrostatic pressure corresponding to this transition is about 0.06 GPa according to Fig. 5b. This strain-induced FM-AFM transition can also happen with a uniaxial strain by changing the out-of-plane lattice constant c and keeping the volume of the unit cell invariant. According to the result shown in Fig. 5d&e, the sign of $E_{AF} - E_{FM}$ shifts from positive to negative when c is changed by about 1.4%; the corresponding compressive pressure in that direction is also about 0.06 GPa.

Since the [Mn₃]-dimer is linked covalently by the linker dpd²⁻, the mechanism of the magnetic interaction is dominated by *collective exchange*, which is sensitive to both bond length and bond angle. Fig. 5c shows the distance between two [Mn₃] planes and the C-C-C bond angle of the linker dpd as a function of strain. As both isotropic and uniaxial compressive strain increases, the magnitude of the bond angle and the distance decreases with an almost linear relation. At the transition point, the distance between two [Mn₃] planes is 6.198 Å under isotropic strain, 0.14% closer than the zero pressure value. The number under uniaxial strain is 6.192 Å, 0.24% closer than the zero-pressure case. On the other hand, the C-C-C bond angle of the linker dpd is 112.94°, 0.13% smaller than for zero pressure. The number under uniaxial strain is 112.99°, 0.09% smaller than zero pressure. The percentage of the change of both distances and bond angles are much

smaller than the percentage of the applied strain, indicating that the major response to strain is the changing of inter-molecular distances instead of the modification of the bond lengths and angles within one $[\text{Mn}_3]$ -dimer molecule. However, this small change is enough to drive the FM-AFM transition, reflecting the sensitivity of the response to the magnetic exchange interaction and confirming the collective-exchange feature.

In summary, we have studied the electronic and magnetic properties of a series of SMM $[\text{Mn}_3]_2$

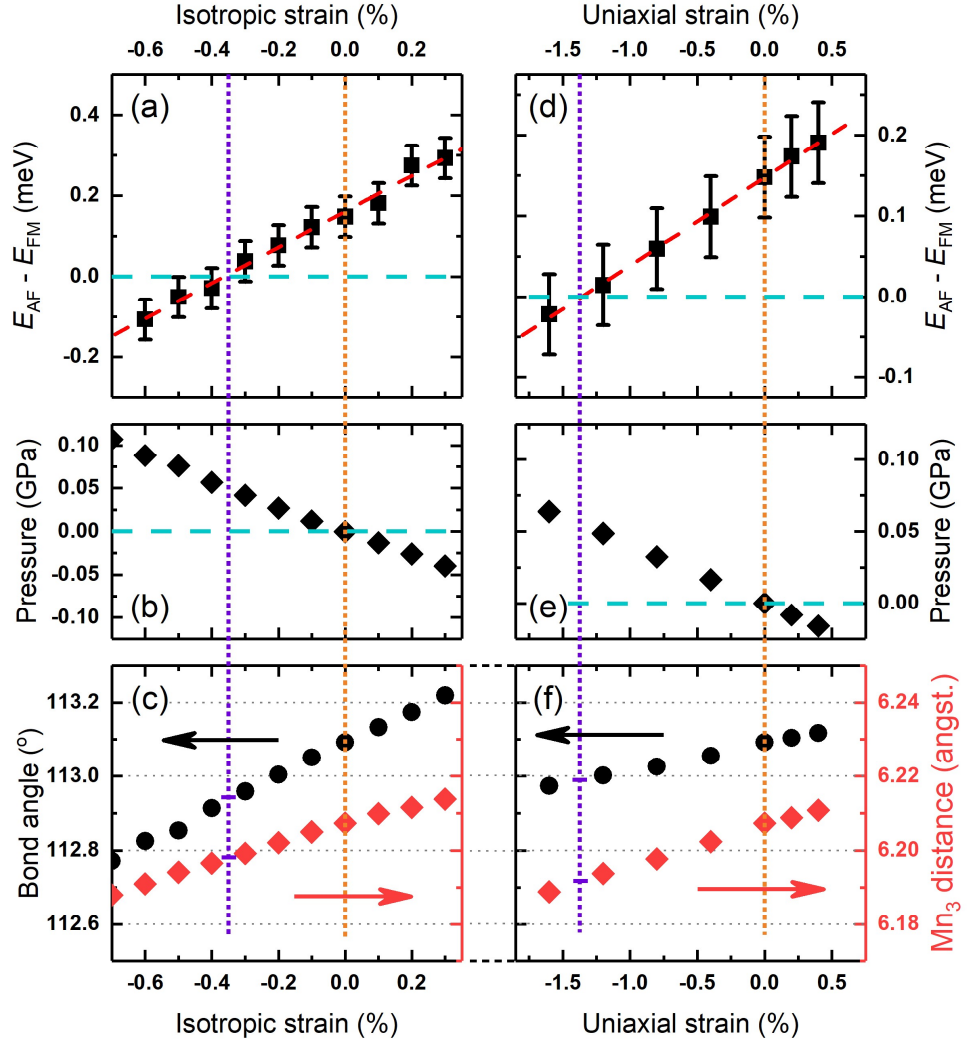


Fig. 5 Strain dependences for $([\text{Mn}_3]_2\text{-}(dpd)_3)_2(\text{I}_3)_4$ bulk. (a) Energy difference $E_{AF} - E_{FM}$ per dimer, (b) pressure, (c) C-C-C bond angle (black dots) of the linker (dpd) and distance (red dots) between two $[\text{Mn}_3]$ as a function of isotropic strain. (d), (e), (f) Similar results as a function of uniaxial strain. (c) and (f) share the same vertical scales. Violet and orange vertical dotted lines represent FM/AF transitions and the unstrained results respectively.

dimers based on first-principles calculations. While energetic determination of the magnetic order

of dimers relies on experiments due to the weak coupling nature, the coupling pathway can be uncovered by Wannier orbital analysis. Total DOS and PDOS results show similar electronic structures of Mn(3d) orbitals among the three dimers. By downfolding into a Mn-centered WF basis, the tight-binding Hamiltonian indicates that only $([Mn_3]_2\text{-}(dpd)_3)^{2+}$ has significant inter-Mn₃ hopping via O₂CMe ligands sufficient to bring about FM coupling. The other two [Mn₃]-dimers, $([Mn_3]_2\text{-}(ppmd)_3)^{2+}$ and $([Mn_3]_2\text{-}(ada)_3)^{2+}$, have small hopping coefficients, via covalently bonded linkers, leading to a much weaker exchange interaction. These results suggest that, like linkers, van der Waals bonded ligands can also affect the sign and strength of magnetic exchange. The calculated results also show that even though the isolated dimer model is different in structure from the bulk form, the trend in the relative energies and densities of states are the same. It is a reasonable model for Wannier function analysis. Finally, the strain dependence of magnetic interactions in the bulk phase of $([Mn_3]_2\text{-}(dpd)_3)_2(I_3)_4$ are investigated under both hydrostatic and uniaxial pressure. A strain-induced FM-AFM transition is identified when an external pressure of about 0.06 GPa is applied, indicating the sensitivity of the response to magnetic exchange interaction and providing potential application to molecular-based spintronics. Experimental work on pressure dependence is underway.

*hping@ufl.edu

Acknowledgment: This work was supported as part of the Center for Molecular Magnetic Quantum Materials, an Energy Frontier Research Center funded by the U.S. Department of Energy, Office of Science, Basic Energy Sciences under Award No. DE-SC0019330. Computations were performed at NERSC and UFRC.

1. Leuenberger, M. N.; Loss, D., Quantum Computing in Molecular Magnets. *Nature* **2001**, *410*, 789-793.
2. Gaita-Arino, A.; Luis, F.; Hill, S.; Coronado, E., Molecular Spins for Quantum Computation. *Nature Chemistry* **2019**, *11*, 301-309.
3. Ding, Y. S.; Yu, K. X.; Reta, D.; Ortu, F.; Winpenny, R. E. P.; Zheng, Y. Z.; Chilton, N. F., Field- and Temperature-Dependent Quantum Tunnelling of the Magnetisation in a Large Barrier Single-Molecule Magnet. *Nature Communications* **2018**, *9*, 10.
4. von Kugelgen, S.; Freedman, D. E., A Chemical Path to Quantum Information. *Science* **2019**, *366*, 1070-1071.
5. Hymas, K.; Soncini, A., Molecular Spintronics Using Single-Molecule Magnets under Irradiation. *Physical Review B* **2019**, *99*.
6. Bogani, L.; Wernsdorfer, W., Molecular Spintronics Using Single-Molecule Magnets. *Nature Materials* **2008**, *7*, 179-186.
7. Wernsdorfer, W.; Bhaduri, S.; Tiron, R.; Hendrickson, D. N.; Christou, G., Spin-Spin Cross Relaxation in Single-Molecule Magnets. *Phys. Rev. Lett.* **2002**, *89*.
8. Wu, Y.-N.; Zhang, X. G.; Cheng, H.-P., Giant Molecular Magnetocapacitance. *Phys. Rev. Lett.* **2013**, *110*, 217205 (5 pages).
9. Thomas, L.; Lointi, F.; Ballou, R.; Gatteschi, D.; Sessoli, R.; Barbara, B., Macroscopic Quantum Tunnelling of Magnetization in a Single Crystal of Nanomagnets. *Nature* **1996**, *383*, 145-147.
10. Nguyen, T. N.; Wernsdorfer, W.; Abboud, K. A.; Christou, G., A Supramolecular Aggregate of Four Exchange-Biased Single-Molecule Magnets. *Journal of the American Chemical Society* **2011**, *133*, 20688-20691.

11. Aubin, S. M. J.; Sun, Z. M.; Pardi, L.; Krzystek, J.; Folting, K.; Brunel, L. C.; Rheingold, A. L.; Christou, G.; Hendrickson, D. N., Reduced Anionic Mn-12 Molecules with Half-Integer Ground States as Single-Molecule Magnets. *Inorganic Chemistry* **1999**, *38*, 5329-5340.
12. Gatteschi, D.; Sessoli, R., Quantum Tunneling of Magnetization and Related Phenomena in Molecular Materials. *Angew Chem Int Edit* **2003**, *42*, 268-297.
13. Guo, Y. N.; Xu, G. F.; Wernsdorfer, W.; Ungur, L.; Guo, Y.; Tang, J. K.; Zhang, H. J.; Chibotaru, L. F.; Powell, A. K., Strong Axiality and Ising Exchange Interaction Suppress Zero-Field Tunneling of Magnetization of an Asymmetric Dy-2 Single-Molecule Magnet. *Journal of the American Chemical Society* **2011**, *133*, 11948-11951.
14. Stamatatos, T. C.; Foguet-Albiol, D.; Lee, S. C.; Stoumpos, C. C.; Raptopoulou, C. P.; Terzis, A.; Wernsdorfer, W.; Hill, S. O.; Perlepes, S. P.; Christou, G., "Switching on" the Properties of Single-Molecule Magnetism in Triangular Manganese(Iii) Complexes. *Journal of the American Chemical Society* **2007**, *129*, 9484-9499.
15. Nguyen, T. N.; Shiddiq, M.; Ghosh, T.; Abboud, K. A.; Hill, S.; Christou, G., Covalently Linked Dimer of Mn-3 Single-Molecule Magnets and Retention of Its Structure and Quantum Properties in Solution. *Journal of the American Chemical Society* **2015**, *137*, 7160-7168.
16. Torikachvili, M. S.; Bud'ko, S. L.; Ni, N.; Canfield, P. C., Pressure Induced Superconductivity in CaFe(2)as(2). *Phys. Rev. Lett.* **2008**, *101*, 057006.
17. Kimura, N.; Ito, K.; Saitoh, K.; Umeda, Y.; Aoki, H.; Terashima, T., Pressure-Induced Superconductivity in Noncentrosymmetric Heavy-Fermion Cerhs13. *Phys. Rev. Lett.* **2005**, *95*, 247004.
18. Radaelli, P. G.; Iannone, G.; Marezio, M.; Hwang, H. Y.; Cheong, S. W.; Jorgensen, J. D.; Argyriou, D. N., Structural Effects on the Magnetic and Transport Properties of Perovskite a(1-X)a(X)'Mno3 (X=0.25, 0.30). *Physical Review B* **1997**, *56*, 8265-8276.
19. Moritomo, Y.; Kuwahara, H.; Tomioka, Y.; Tokura, Y., Pressure Effects on Charge-Ordering Transitions in Perovskite Manganites. *Physical Review B* **1997**, *55*, 7549-7556.
20. Trimarchi, G.; Binggeli, N., Structural and Electronic Properties of Lamno3 under Pressure: An Ab Initio Lda+U Study. *Physical Review B* **2005**, *71*.
21. Pinsard-Gaudart, L.; Rodriguez-Carvajal, J.; Daoud-Aladine, A.; Goncharenko, I.; Medarde, M.; Smith, R. L.; Revcolevschi, A., Stability of the Jahn-Teller Effect and Magnetic Study of Lamno3 under Pressure. *Physical Review B* **2001**, *64*.
22. Woodall, C. H., et al., Pressure Induced Enhancement of the Magnetic Ordering Temperature in Rhenium(Iv) Monomers. *Nature Communications* **2016**, *7*, 7.
23. Atkinson, J. H.; Fournet, A. D.; Bhaskaran, L.; Myasoedov, Y.; Zeldov, E.; del Barco, E.; Hill, S.; Christou, G.; Friedman, J. R., Effects of Uniaxial Pressure on the Quantum Tunneling of Magnetization in a High-Symmetry Mn-12 Single-Molecule Magnet. *Physical Review B* **2017**, *95*, 11.
24. Foss-Feig, M. S.; Friedman, J. R., Geometric-Phase-Effect Tunnel-Splitting Oscillations in Single-Molecule Magnets with Fourth-Order Anisotropy Induced by Orthorhombic Distortion. *Epl* **2009**, *86*, 6.
25. Seikh, M. M.; Caignaert, V.; Perez, O.; Raveau, B.; Hardy, V., Interplay between Single-Ion Magnetism, Single-Chain Magnetism and Long-Range Ordering in the Spin Chain Oxides Sr4-Xcaxmn2coo9. *J. Mater. Chem. C* **2018**, *6*, 3362-3372.
26. Cao, T. S.; Chen, D.-T.; Abboud, K. A.; Zhang, X. G.; Cheng, H.-P.; Christou, G., Feasibility of Ground State Spin Switching in a Molecular Analogue of the Mixed-Metal Oxides with the Perovskite Structure. *Polyhedron* **2019**.
27. Kohn, W.; Sham, L. J., Self-Consistent Equations Including Exchange and Correlation Effects. *Phys Rev* **1965**, *140*, A1133-A1138.
28. Perdew, J. P.; Burke, K.; Ernzerhof, M., Generalized Gradient Approximation Made Simple. *Phys. Rev. Lett.* **1996**, *77*, 3865-3868.
29. Bl; ouml; chl, P. E., Projector Augmented-Wave Method. *Physical Review B* **1994**, *50*, 17953.
30. Furthmüller, K. a. J., Vasp. *VASP (Institut für Materialphysik, Universität Wien, Vienna, Austria, 1999)*.

31. LIECHTENSTEIN, A.; ANISIMOV, V.; ZAANEN, J., Density-Functional Theory and Strong-Interactions - Orbital Ordering in Mott-Hubbard Insulators. *Physical Review B* **1995**, *52*, R5467-R5470.
32. Vaugier, L.; Jiang, H.; Biermann, S., Hubbard U and Hund Exchange J in Transition Metal Oxides: Screening Versus Localization Trends from Constrained Random Phase Approximation. *Physical Review B* **2012**, *86*, 165105.
33. Grimme, S.; Antony, J.; Ehrlich, S.; Krieg, H., A Consistent and Accurate Ab Initio Parametrization of Density Functional Dispersion Correction (Dft-D) for the 94 Elements H-Pu. *Journal of Chemical Physics* **2010**, *132*.
34. Marzari, N.; Vanderbilt, D., Maximally Localized Generalized Wannier Functions for Composite Energy Bands. *Physical Review B* **1997**, *56*, 12847-12865.
35. Mostofi, A. A.; Yates, J. R.; Lee, Y. S.; Souza, I.; Vanderbilt, D.; Marzari, N., Wannier90: A Tool for Obtaining Maximally-Localised Wannier Functions. *Comput. Phys. Commun.* **2008**, *178*, 685-699.
36. Li, T. X., et al., Pressure-Controlled Interlayer Magnetism in Atomically Thin Cri3. *Nature Materials* **2019**, *18*, 1303-+.

Supplementary Materials for “Analysis of exchange interactions in dimers of Mn₃ single-molecule magnets, and their sensitivity to external pressure”

Jie-Xiang Yu^{1,2,3}, George Christou^{2,4} and Hai-Ping Cheng^{1,2,4*}

¹Department of Physics, ²The M²QM Center, ³The Quantum Theory Project

and ⁴Department of Chemistry, University of Florida, Gainesville, FL, USA

1. Hubbard U -dependent calculations

The inter-[Mn₃] magnetic interaction in the ([Mn₃]₂-(dpd)₃)²⁺ dimer is a very weak inter-unit ferromagnetic coupling, with $J \approx 0.025$ cm⁻¹ according to EPR measurements [Ref. 15 in the main text]. Considering spin states $S = 6$ for each [Mn₃] monomer, we know that the energy difference $E_{AF} - E_{FM}$ between inter-[Mn₃] FM and AFM spin configurations per dimer is about 0.2 meV. Since the exchange coupling is usually highly influenced by Hubbard U , it is necessary to choose a reasonable value of Hubbard U . Therefore, we calculate $E_{AF} - E_{FM}$ as a function of U for a [Mn₃]₂ crystal. Without U , $E_{AF} - E_{FM} = -2.48$ meV; $E_{AF} - E_{FM} = -0.37$ meV at $U = 2.5$ eV; $E_{AF} - E_{FM} = 0.41$ meV at $U = 3.0$ eV; $E_{AF} - E_{FM} = 1.65$ meV at $U = 4.0$ eV. In this case, $E_{AF} - E_{FM} = 0.13$ meV at $U = 2.8$ eV best matches the experimental result and we use this U value in the rest of our calculations.

2. Downfolding and Mn-centered WF-based Hamiltonian

As mentioned in the main text, we use the MLWF method to get the WF-based Hamiltonian with Mn(3d) orbitals as the initial projections of Wannier functions for the downfolding process. As a result, thirty WFs are obtained, where five WFs are centered on the same Mn. We focus on the inter-Mn₃ hopping of the Hamiltonian between two sets of five WFs, one centered on the Mn on the left side of the dimer and the other centered on the Mn on the right side.

([Mn₃]₂-(dpd)₃)²⁺: the inter-Mn₃ matrix element or hopping coefficient t_{lr} between Mn-centered WF in the spin-majority channel, in units of eV:

t_{lr}	$ W1_r^o\rangle$	$ W2_r^o\rangle$	$ W3_r^o\rangle$	$ W4_r^o\rangle$	$ W5_r^u\rangle$
$\langle W1_l^o $	-0.005	0.004	-0.032	-0.011	-0.033
$\langle W2_l^o $	-0.004	-0.004	-0.047	-0.011	-0.001
$\langle W3_l^o $	-0.032	0.044	0.003	-0.003	0.070
$\langle W4_l^o $	0.012	-0.004	-0.002	-0.001	-0.005
$\langle W5_l^u $	-0.032	-0.008	0.068	0.011	0.043

Labels W1 to W5 are the same as in the main text. Subscripts l and r represent the left and right side of the dimer respectively. Superscripts o and u represent occupied and unoccupied WFs respectively. Bold numbers are the hopping between occupied and unoccupied WFs, and red shows the strongest ones. The corresponding full Hamiltonian matrix appears at the end of the document.

Similar matrix elements for $([\text{Mn}_3]_2\text{-}(\text{ppmd})_3)^{2+}$ are given by:

t_{lr}	$ W1_r^o\rangle$	$ W2_r^o\rangle$	$ W3_r^o\rangle$	$ W4_r^o\rangle$	$ W5_r^u\rangle$
$\langle W1_l^o $	0.000	0.000	0.000	-0.002	0.002
$\langle W2_l^o $	0.000	0.000	-0.006	-0.001	0.002
$\langle W3_l^o $	0.004	-0.004	0.008	-0.006	-0.018
$\langle W4_l^o $	-0.002	0.000	0.006	0.002	0.005
$\langle W5_l^u $	-0.003	0.000	-0.019	-0.004	-0.016

The corresponding full Hamiltonian matrix appears at the end of the document.

For $([\text{Mn}_3]_2\text{-}(\text{ada})_3)^{2+}$ in the AFM spin configuration, we let Mn on the left side of the dimer (Fig. 4(c) in the main text) be spin-up, so that in the spin-majority channel, four of five Mn-centered WFs are occupied on the left side while all Mn-center WFs are unoccupied at the right side. Thus, the corresponding inter-Mn₃ hopping t_{lr} is given by:

t_{lr}	$ W1_r^u\rangle$	$ W2_r^u\rangle$	$ W3_r^u\rangle$	$ W4_r^u\rangle$	$ W5_r^u\rangle$
$\langle W1_l^o $	0.001	0.001	0.000	-0.001	0.000
$\langle W2_l^o $	-0.001	0.001	0.000	0.000	-0.001
$\langle W3_l^o $	-0.002	0.003	0.001	-0.002	-0.015
$\langle W4_l^o $	-0.004	0.002	0.001	0.005	-0.003
$\langle W5_l^u $	0.001	0.001	-0.001	-0.001	0.000

Again, the corresponding full Hamiltonian matrix appears at the end of the document.

3. Projected density-of-state of linkers

The PDOS of the linkers of three [Mn₃]-dimers are shown in Fig. S1. For $([\text{Mn}_3]_2\text{-}(\text{dpd})_3)^{2+}$, the component of dpd are mainly at -6~-4 eV which is far from the Fermi level. On the other hand, the component of ppmd in $([\text{Mn}_3]_2\text{-}(\text{ppmd})_3)^{2+}$ and that of ada in $([\text{Mn}_3]_2\text{-}(\text{ada})_3)^{2+}$ has significant features at -2~-1 eV which is near the Fermi level. To this end, the linker dpd are not involved into the exchange pathway while the linkers ppmd and ada play key roles on exchange interaction.

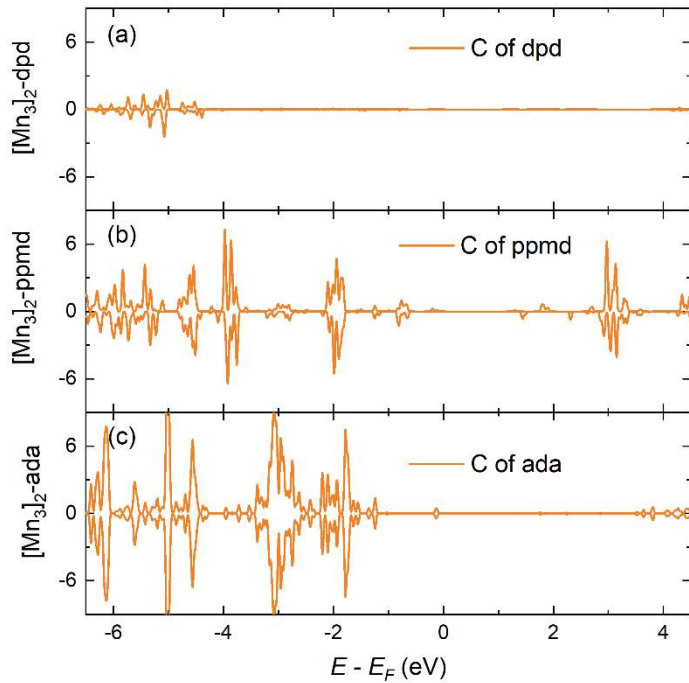


Fig. S1 In their gas phases, the PDOS of 2s and 2p orbitals of (a) the carbon of dpd, (b) six carbons of ppmd and (c) ten carbons of ada.

4. Alternative WF-based Hamiltonian near the Fermi level

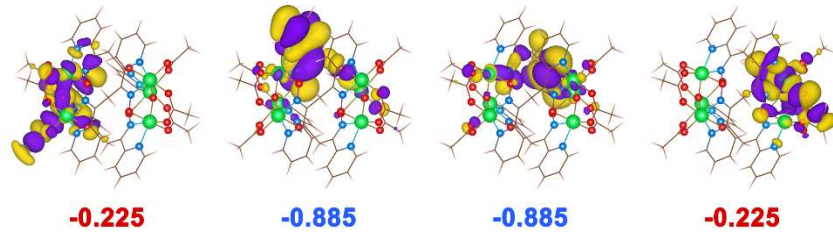


Fig. S2 Four of the WFs obtained from the top fourteen occupied eigenstates in $([Mn_3]_2\text{-}(dpd)_3)^{2+}$ near the Fermi level. Red and blue numbers represent the on-site energies relative to the Fermi level in units of eV for two Mn-centered and two O₂CMe ligand-dominated WFs respectively.

To see clearly what local orbitals are associated with the sub-HOMO states, that is, the hybridization of ligand orbitals and Mn(3d) orbitals that dominate HOMO/LUMO levels in dimer systems, circled by green dashed line in Fig. 2 in the main text, we use a gas phase model $([Mn_3]_2\text{-}(dpd)_3)^{2+}$ to perform a unitary transformation on Bloch waves near the Fermi level. This time, we use both Mn(3d) and ligand orbitals as base functions without downfolding. The eigenvalues of the WF-based tight-binding Hamiltonian can reproduce the eigenvalues obtained by DFT.

The top fourteen occupied eigenstates in the spin-majority channel are included in the energy window. As a result, fourteen corresponding MLWFs are obtained. Fig. S2 shows four typical WFs. Two of them, with lower on-site energies, display significant features of O₂CMe ligands, indicating that the sub-HOMO states are dominated by O₂CMe ligands. Compared to the

Mn(3d)-only WF construction which gives an *effective* Hamiltonian for long-range *collective-exchange*, this Wannier transformation demonstrates the physical processes and channels for exchange coupling between the two [Mn₃] monomers.

5. Density-of-state results for ([Mn₃]₂-(dpd)₃)₂(I₃)₄ bulk

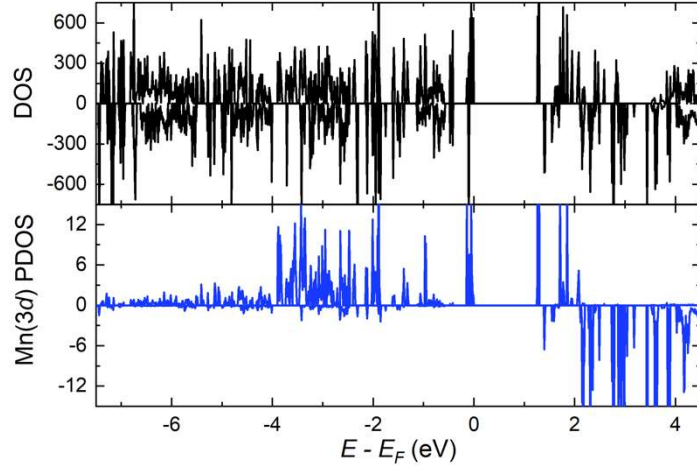


Fig. S3 the total DOS and PDOS of Mn(3d) orbitals in the bulk phase of ([Mn₃]₂-(dpd)₃)₂(I₃)₄.

DOS and PDOS in the bulk phase of ([Mn₃]₂-(dpd)₃)₂(I₃)₄ (shown in Fig. S3) gives very the same electronic structure as that in the gas phase.

Appendix: Tight-binding Hamiltonian

The matrix elements of the three Mn-centered tight-binding Hamiltonians are listed below in three sets of columns. In each set, the first and second column are the indices of the WFs and the third column is the matrix element of the Hamiltonian. For ($[\text{Mn}_3]_2\text{-}(\text{dpd})_3$) $^{2+}$ and ($[\text{Mn}_3]_2\text{-}(\text{ppmd})_3$) $^{2+}$, orbitals 1~5, 6~10, and 11~15 are three sets of WFs centered on three Mn atoms on the left side of the dimer; 16~20, 21~25, 26~30 are three sets of WFs centered on three Mn atoms on the right side. For ($[\text{Mn}_3]_2\text{-}(\text{ada})_3$) $^{2+}$, orbitals 1~5, 11~15, and 21~25 are WFs centered on the three spin-up Mn atoms at the left side, and 6~10, 16~20, 26~30 are centered on the three spin-down Mn atoms at the right side. WFs with similar on-site energies are classified into the same label. For example, Nos. 1, 10, 11, 16, 21 and 30 in ($[\text{Mn}_3]_2\text{-}(\text{dpd})_3$) $^{2+}$ have the lowest on-site energies among their five WFs centered on the corresponding Mn, so they are all labeled by WF1 in the main text.

Tight-binding Hamiltonian of ($[\text{Mn}_3]_2\text{-}(\text{dpd})_3$) $^{2+}$

1	1	-8.225	1	11	-0.014	1	21	0.002
2	1	0.190	2	11	-0.008	2	21	0.008
3	1	0.050	3	11	-0.086	3	21	0.034
4	1	-0.052	4	11	-0.173	4	21	0.005
5	1	-0.077	5	11	0.066	5	21	0.001
6	1	-0.056	6	11	-0.028	6	21	0.006
7	1	0.061	7	11	-0.037	7	21	0.036
8	1	-0.010	8	11	-0.127	8	21	0.035
9	1	0.088	9	11	-0.263	9	21	-0.020
10	1	-0.031	10	11	-0.030	10	21	0.003
11	1	-0.014	11	11	-8.265	11	21	-0.005
12	1	0.130	12	11	0.030	12	21	0.032
13	1	-0.039	13	11	-0.109	13	21	0.033
14	1	-0.035	14	11	0.043	14	21	-0.004
15	1	0.175	15	11	-0.152	15	21	-0.012
16	1	-0.005	16	11	-0.001	16	21	-0.014
17	1	-0.032	17	11	-0.023	17	21	0.039
18	1	-0.032	18	11	0.029	18	21	-0.130
19	1	-0.004	19	11	0.004	19	21	-0.034
20	1	0.012	20	11	-0.016	20	21	-0.173
21	1	0.002	21	11	-0.005	21	21	-8.228
22	1	0.008	22	11	-0.033	22	21	0.192
23	1	-0.035	23	11	0.016	23	21	-0.048
24	1	0.005	24	11	-0.011	24	21	-0.051
25	1	-0.001	25	11	-0.004	25	21	0.077
26	1	0.006	26	11	0.002	26	21	-0.056
27	1	0.036	27	11	-0.030	27	21	0.060
28	1	-0.035	28	11	-0.008	28	21	0.010
29	1	-0.020	29	11	-0.004	29	21	0.087
30	1	-0.003	30	11	0.001	30	21	0.031
1	2	0.190	1	12	0.130	1	22	0.008

2	2	-3.517	2	12	-0.013	2	22	-0.002
3	2	-0.006	3	12	0.042	3	22	-0.001
4	2	0.025	4	12	0.026	4	22	-0.004
5	2	-0.674	5	12	0.012	5	22	0.002
6	2	-0.096	6	12	0.009	6	22	0.032
7	2	0.045	7	12	0.037	7	22	-0.040
8	2	0.014	8	12	-0.013	8	22	-0.044
9	2	0.026	9	12	-0.014	9	22	0.066
10	2	0.089	10	12	-0.005	10	22	-0.013
11	2	-0.008	11	12	0.030	11	22	-0.033
12	2	-0.013	12	12	-3.513	12	22	-0.043
13	2	-0.037	13	12	0.001	13	22	-0.070
14	2	-0.004	14	12	-0.670	14	22	-0.001
15	2	-0.016	15	12	-0.024	15	22	0.005
16	2	-0.033	16	12	-0.029	16	22	-0.008
17	2	0.070	17	12	-0.035	17	22	0.037
18	2	0.043	18	12	0.043	18	22	0.013
19	2	-0.001	19	12	-0.021	19	22	-0.004
20	2	-0.005	20	12	-0.068	20	22	0.016
21	2	0.008	21	12	0.032	21	22	0.192
22	2	-0.002	22	12	-0.043	22	22	-3.520
23	2	0.001	23	12	0.068	23	22	0.005
24	2	-0.004	24	12	-0.011	24	22	0.025
25	2	-0.002	25	12	-0.008	25	22	0.673
26	2	0.032	26	12	-0.005	26	22	-0.096
27	2	-0.041	27	12	-0.001	27	22	0.045
28	2	0.044	28	12	-0.002	28	22	-0.014
29	2	0.066	29	12	-0.004	29	22	0.027
30	2	0.013	30	12	-0.006	30	22	-0.089
1	3	0.050	1	13	-0.039	1	23	-0.035
2	3	-0.006	2	13	-0.037	2	23	0.001
3	3	-5.136	3	13	-0.096	3	23	-0.004
4	3	-0.293	4	13	-0.040	4	23	-0.010
5	3	0.187	5	13	-0.053	5	23	0.009
6	3	-0.001	6	13	-0.033	6	23	0.045
7	3	-0.137	7	13	0.130	7	23	-0.014
8	3	0.038	8	13	0.044	8	23	-0.042
9	3	-0.063	9	13	-0.450	9	23	-0.005
10	3	-0.039	10	13	-0.146	10	23	-0.001
11	3	-0.086	11	13	-0.109	11	23	0.016
12	3	0.042	12	13	0.001	12	23	0.068
13	3	-0.096	13	13	-5.181	13	23	0.003
14	3	0.085	14	13	0.155	14	23	0.048
15	3	-0.430	15	13	0.168	15	23	-0.002
16	3	-0.016	16	13	0.023	16	23	0.086

17	3	0.003	17	13	0.015	17	23	-0.097
18	3	0.068	18	13	-0.035	18	23	0.042
19	3	-0.047	19	13	0.037	19	23	-0.085
20	3	-0.002	20	13	-0.004	20	23	-0.431
21	3	0.034	21	13	0.033	21	23	-0.048
22	3	-0.001	22	13	-0.070	22	23	0.005
23	3	-0.004	23	13	0.003	23	23	-5.140
24	3	0.010	24	13	-0.003	24	23	0.291
25	3	0.009	25	13	0.044	25	23	0.188
26	3	-0.045	26	13	-0.033	26	23	0.001
27	3	0.014	27	13	0.005	27	23	0.136
28	3	-0.042	28	13	-0.002	28	23	0.038
29	3	0.005	29	13	0.010	29	23	0.063
30	3	-0.001	30	13	-0.015	30	23	-0.040
1	4	-0.052	1	14	-0.035	1	24	0.005
2	4	0.025	2	14	-0.004	2	24	-0.004
3	4	-0.293	3	14	0.085	3	24	0.010
4	4	-3.844	4	14	0.244	4	24	-0.002
5	4	-0.177	5	14	-0.022	5	24	0.002
6	4	-0.048	6	14	-0.028	6	24	0.024
7	4	0.426	7	14	0.026	7	24	0.006
8	4	-0.014	8	14	-0.031	8	24	-0.064
9	4	0.277	9	14	0.221	9	24	-0.009
10	4	-0.344	10	14	0.065	10	24	-0.001
11	4	-0.173	11	14	0.043	11	24	-0.011
12	4	0.026	12	14	-0.670	12	24	-0.011
13	4	-0.040	13	14	0.155	13	24	-0.003
14	4	0.244	14	14	-8.166	14	24	-0.011
15	4	-0.295	15	14	0.171	15	24	-0.001
16	4	-0.011	16	14	0.004	16	24	-0.173
17	4	0.003	17	14	-0.037	17	24	0.040
18	4	0.011	18	14	0.021	18	24	-0.026
19	4	-0.011	19	14	0.008	19	24	0.243
20	4	0.001	20	14	-0.023	20	24	0.294
21	4	0.005	21	14	-0.004	21	24	-0.051
22	4	-0.004	22	14	-0.001	22	24	0.025
23	4	-0.010	23	14	0.048	23	24	0.291
24	4	-0.002	24	14	-0.011	24	24	-3.846
25	4	-0.002	25	14	0.003	25	24	0.178
26	4	0.024	26	14	-0.001	26	24	-0.050
27	4	0.006	27	14	-0.020	27	24	0.425
28	4	0.064	28	14	-0.001	28	24	0.014
29	4	-0.009	29	14	0.001	29	24	0.277
30	4	0.001	30	14	0.001	30	24	0.344
1	5	-0.077	1	15	0.175	1	25	-0.001

2	5	-0.674	2	15	-0.016	2	25	-0.002
3	5	0.187	3	15	-0.430	3	25	0.009
4	5	-0.177	4	15	-0.295	4	25	-0.002
5	5	-8.180	5	15	0.287	5	25	0.001
6	5	-0.003	6	15	0.108	6	25	0.009
7	5	0.113	7	15	-0.045	7	25	0.030
8	5	0.001	8	15	-0.021	8	25	0.015
9	5	0.285	9	15	0.248	9	25	-0.016
10	5	-0.057	10	15	0.266	10	25	0.000
11	5	0.066	11	15	-0.152	11	25	-0.004
12	5	0.012	12	15	-0.024	12	25	-0.008
13	5	-0.053	13	15	0.168	13	25	0.044
14	5	-0.022	14	15	0.171	14	25	0.003
15	5	0.287	15	15	-3.806	15	25	-0.004
16	5	0.004	16	15	0.016	16	25	-0.066
17	5	0.044	17	15	-0.004	17	25	-0.053
18	5	-0.008	18	15	-0.068	18	25	0.013
19	5	-0.003	19	15	0.023	19	25	0.022
20	5	-0.004	20	15	-0.010	20	25	0.287
21	5	0.001	21	15	-0.012	21	25	0.077
22	5	0.002	22	15	0.005	22	25	0.673
23	5	0.009	23	15	-0.002	23	25	0.188
24	5	0.002	24	15	-0.001	24	25	0.178
25	5	0.001	25	15	-0.004	25	25	-8.185
26	5	-0.009	26	15	0.000	26	25	0.003
27	5	-0.030	27	15	-0.010	27	25	-0.113
28	5	0.015	28	15	0.003	28	25	0.001
29	5	0.016	29	15	0.003	29	25	-0.285
30	5	0.000	30	15	0.003	30	25	-0.057
1	6	-0.056	1	16	-0.005	1	26	0.006
2	6	-0.096	2	16	-0.033	2	26	0.032
3	6	-0.001	3	16	-0.016	3	26	-0.045
4	6	-0.048	4	16	-0.011	4	26	0.024
5	6	-0.003	5	16	0.004	5	26	-0.009
6	6	-8.158	6	16	0.002	6	26	-0.004
7	6	0.081	7	16	-0.030	7	26	0.049
8	6	0.547	8	16	0.008	8	26	-0.017
9	6	-0.086	9	16	-0.004	9	26	0.014
10	6	0.020	10	16	-0.001	10	26	0.004
11	6	-0.028	11	16	-0.001	11	26	0.002
12	6	0.009	12	16	-0.029	12	26	-0.005
13	6	-0.033	13	16	0.023	13	26	-0.033
14	6	-0.028	14	16	0.004	14	26	-0.001
15	6	0.108	15	16	0.016	15	26	0.000
16	6	0.002	16	16	-8.263	16	26	-0.028

17	6	0.033	17	16	0.109	17	26	0.034
18	6	0.005	18	16	-0.030	18	26	-0.009
19	6	-0.001	19	16	0.043	19	26	-0.028
20	6	0.000	20	16	0.154	20	26	-0.109
21	6	0.006	21	16	-0.014	21	26	-0.056
22	6	0.032	22	16	-0.008	22	26	-0.096
23	6	0.045	23	16	0.086	23	26	0.001
24	6	0.024	24	16	-0.173	24	26	-0.050
25	6	0.009	25	16	-0.066	25	26	0.003
26	6	-0.004	26	16	-0.028	26	26	-8.156
27	6	0.048	27	16	-0.036	27	26	0.081
28	6	0.017	28	16	0.127	28	26	-0.549
29	6	0.014	29	16	-0.263	29	26	-0.085
30	6	-0.004	30	16	0.030	30	26	-0.020
1	7	0.061	1	17	-0.032	1	27	0.036
2	7	0.045	2	17	0.070	2	27	-0.041
3	7	-0.137	3	17	0.003	3	27	0.014
4	7	0.426	4	17	0.003	4	27	0.006
5	7	0.113	5	17	0.044	5	27	-0.030
6	7	0.081	6	17	0.033	6	27	0.048
7	7	-5.148	7	17	-0.005	7	27	0.003
8	7	0.004	8	17	-0.002	8	27	-0.069
9	7	-0.263	9	17	-0.010	9	27	0.003
10	7	0.169	10	17	-0.015	10	27	0.011
11	7	-0.037	11	17	-0.023	11	27	-0.030
12	7	0.037	12	17	-0.035	12	27	-0.001
13	7	0.130	13	17	0.015	13	27	0.005
14	7	0.026	14	17	-0.037	14	27	-0.020
15	7	-0.045	15	17	-0.004	15	27	-0.010
16	7	-0.030	16	17	0.109	16	27	-0.036
17	7	-0.005	17	17	-5.179	17	27	-0.131
18	7	0.001	18	17	0.001	18	27	-0.037
19	7	-0.020	19	17	-0.156	19	27	0.026
20	7	0.010	20	17	0.168	20	27	0.046
21	7	0.036	21	17	0.039	21	27	0.060
22	7	-0.040	22	17	0.037	22	27	0.045
23	7	-0.014	23	17	-0.097	23	27	0.136
24	7	0.006	24	17	0.040	24	27	0.425
25	7	0.030	25	17	-0.053	25	27	-0.113
26	7	0.049	26	17	0.034	26	27	0.081
27	7	0.003	27	17	-0.131	27	27	-5.147
28	7	0.069	28	17	0.044	28	27	-0.004
29	7	0.003	29	17	0.450	29	27	-0.265
30	7	-0.011	30	17	-0.145	30	27	-0.168
1	8	-0.010	1	18	-0.032	1	28	-0.035

2	8	0.014	2	18	0.043	2	28	0.044
3	8	0.038	3	18	0.068	3	28	-0.042
4	8	-0.014	4	18	0.011	4	28	0.064
5	8	0.001	5	18	-0.008	5	28	0.015
6	8	0.547	6	18	0.005	6	28	0.017
7	8	0.004	7	18	0.001	7	28	0.069
8	8	-3.501	8	18	-0.002	8	28	-0.043
9	8	-0.023	9	18	0.004	9	28	0.009
10	8	0.372	10	18	-0.006	10	28	-0.028
11	8	-0.127	11	18	0.029	11	28	-0.008
12	8	-0.013	12	18	0.043	12	28	-0.002
13	8	0.044	13	18	-0.035	13	28	-0.002
14	8	-0.031	14	18	0.021	14	28	-0.001
15	8	-0.021	15	18	-0.068	15	28	0.003
16	8	0.008	16	18	-0.030	16	28	0.127
17	8	-0.002	17	18	0.001	17	28	0.044
18	8	-0.002	18	18	-3.509	18	28	-0.013
19	8	0.001	19	18	0.670	19	28	0.032
20	8	0.003	20	18	-0.025	20	28	-0.022
21	8	0.035	21	18	-0.130	21	28	0.010
22	8	-0.044	22	18	0.013	22	28	-0.014
23	8	-0.042	23	18	0.042	23	28	0.038
24	8	-0.064	24	18	-0.026	24	28	0.014
25	8	0.015	25	18	0.013	25	28	0.001
26	8	-0.017	26	18	-0.009	26	28	-0.549
27	8	-0.069	27	18	-0.037	27	28	-0.004
28	8	-0.043	28	18	-0.013	28	28	-3.499
29	8	-0.009	29	18	0.014	29	28	0.023
30	8	-0.028	30	18	-0.005	30	28	0.370
1	9	0.088	1	19	-0.004	1	29	-0.020
2	9	0.026	2	19	-0.001	2	29	0.066
3	9	-0.063	3	19	-0.047	3	29	0.005
4	9	0.277	4	19	-0.011	4	29	-0.009
5	9	0.285	5	19	-0.003	5	29	0.016
6	9	-0.086	6	19	-0.001	6	29	0.014
7	9	-0.263	7	19	-0.020	7	29	0.003
8	9	-0.023	8	19	0.001	8	29	-0.009
9	9	-3.833	9	19	0.001	9	29	-0.001
10	9	-0.184	10	19	-0.001	10	29	-0.004
11	9	-0.263	11	19	0.004	11	29	-0.004
12	9	-0.014	12	19	-0.021	12	29	-0.004
13	9	-0.450	13	19	0.037	13	29	0.010
14	9	0.221	14	19	0.008	14	29	0.001
15	9	0.248	15	19	0.023	15	29	0.003
16	9	-0.004	16	19	0.043	16	29	-0.263

17	9	-0.010	17	19	-0.156	17	29	0.450
18	9	0.004	18	19	0.670	18	29	0.014
19	9	0.001	19	19	-8.165	19	29	0.220
20	9	-0.003	20	19	-0.170	20	29	-0.248
21	9	-0.020	21	19	-0.034	21	29	0.087
22	9	0.066	22	19	-0.004	22	29	0.027
23	9	-0.005	23	19	-0.085	23	29	0.063
24	9	-0.009	24	19	0.243	24	29	0.277
25	9	-0.016	25	19	0.022	25	29	-0.285
26	9	0.014	26	19	-0.028	26	29	-0.085
27	9	0.003	27	19	0.026	27	29	-0.265
28	9	0.009	28	19	0.032	28	29	0.023
29	9	-0.001	29	19	0.220	29	29	-3.832
30	9	0.004	30	19	-0.065	30	29	0.183
1	10	-0.031	1	20	0.012	1	30	-0.003
2	10	0.089	2	20	-0.005	2	30	0.013
3	10	-0.039	3	20	-0.002	3	30	-0.001
4	10	-0.344	4	20	0.001	4	30	0.001
5	10	-0.057	5	20	-0.004	5	30	0.000
6	10	0.020	6	20	0.000	6	30	-0.004
7	10	0.169	7	20	0.010	7	30	-0.011
8	10	0.372	8	20	0.003	8	30	-0.028
9	10	-0.184	9	20	-0.003	9	30	0.004
10	10	-8.290	10	20	0.003	10	30	-0.002
11	10	-0.030	11	20	-0.016	11	30	0.001
12	10	-0.005	12	20	-0.068	12	30	-0.006
13	10	-0.146	13	20	-0.004	13	30	-0.015
14	10	0.065	14	20	-0.023	14	30	0.001
15	10	0.266	15	20	-0.010	15	30	0.003
16	10	-0.001	16	20	0.154	16	30	0.030
17	10	-0.015	17	20	0.168	17	30	-0.145
18	10	-0.006	18	20	-0.025	18	30	-0.005
19	10	-0.001	19	20	-0.170	19	30	-0.065
20	10	0.003	20	20	-3.805	20	30	0.265
21	10	0.003	21	20	-0.173	21	30	0.031
22	10	-0.013	22	20	0.016	22	30	-0.089
23	10	-0.001	23	20	-0.431	23	30	-0.040
24	10	-0.001	24	20	0.294	24	30	0.344
25	10	0.000	25	20	0.287	25	30	-0.057
26	10	0.004	26	20	-0.109	26	30	-0.020
27	10	0.011	27	20	0.046	27	30	-0.168
28	10	-0.028	28	20	-0.022	28	30	0.370
29	10	-0.004	29	20	-0.248	29	30	0.183
30	10	-0.002	30	20	0.265	30	30	-8.289

Tight-binding Hamiltonian for ($[\text{Mn}_3]_2\text{-}(\text{ppmd})_3$) $^{2+}$

1	1	-8.085	1	11	-0.019	1	21	0.001
2	1	-0.022	2	11	0.012	2	21	0.000
3	1	-0.552	3	11	0.082	3	21	-0.006
4	1	-0.043	4	11	0.028	4	21	0.000
5	1	0.138	5	11	-0.112	5	21	0.001
6	1	-0.032	6	11	-0.039	6	21	0.000
7	1	-0.041	7	11	-0.060	7	21	-0.002
8	1	-0.025	8	11	-0.010	8	21	0.000
9	1	0.150	9	11	0.019	9	21	0.001
10	1	-0.058	10	11	0.026	10	21	0.000
11	1	-0.019	11	11	-8.069	11	21	0.000
12	1	0.007	12	11	-0.339	12	21	0.000
13	1	0.012	13	11	0.086	13	21	0.004
14	1	0.168	14	11	-0.160	14	21	0.000
15	1	0.016	15	11	0.015	15	21	0.000
16	1	0.000	16	11	0.000	16	21	-0.019
17	1	0.000	17	11	0.000	17	21	0.007
18	1	-0.004	18	11	0.003	18	21	-0.012
19	1	0.000	19	11	-0.002	19	21	0.168
20	1	0.000	20	11	0.000	20	21	-0.016
21	1	0.001	21	11	0.000	21	21	-8.083
22	1	0.006	22	11	-0.002	22	21	0.552
23	1	0.000	23	11	0.006	23	21	0.022
24	1	0.000	24	11	0.000	24	21	-0.043
25	1	-0.001	25	11	0.001	25	21	-0.138
26	1	0.000	26	11	0.001	26	21	-0.032
27	1	-0.002	27	11	0.000	27	21	-0.041
28	1	0.000	28	11	-0.007	28	21	0.026
29	1	0.001	29	11	0.001	29	21	0.150
30	1	0.000	30	11	0.001	30	21	0.057
1	2	-0.022	1	12	0.007	1	22	0.006
2	2	-5.034	2	12	0.041	2	22	0.000
3	2	0.000	3	12	0.011	3	22	0.035
4	2	0.099	4	12	-0.006	4	22	-0.003
5	2	-0.256	5	12	-0.029	5	22	0.002
6	2	0.031	6	12	0.064	6	22	0.000
7	2	-0.137	7	12	0.158	7	22	0.005
8	2	0.156	8	12	-0.011	8	22	0.002
9	2	-0.386	9	12	-0.060	9	22	-0.004
10	2	0.116	10	12	0.072	10	22	0.000
11	2	0.012	11	12	-0.339	11	22	-0.002
12	2	0.041	12	12	-3.271	12	22	0.016
13	2	-0.117	13	12	-0.002	13	22	-0.018

14	2	-0.057	14	12	0.057	14	22	-0.005
15	2	0.063	15	12	-0.449	15	22	0.002
16	2	-0.006	16	12	0.000	16	22	-0.082
17	2	-0.019	17	12	0.002	17	22	-0.011
18	2	0.008	18	12	0.005	18	22	0.153
19	2	0.006	19	12	-0.004	19	22	-0.062
20	2	0.000	20	12	0.000	20	22	-0.054
21	2	0.000	21	12	0.000	21	22	0.552
22	2	0.000	22	12	0.016	22	22	-3.266
23	2	-0.003	23	12	0.019	23	22	0.000
24	2	0.000	24	12	-0.003	24	22	0.111
25	2	0.001	25	12	0.004	25	22	-0.054
26	2	0.003	26	12	-0.007	26	22	-0.010
27	2	0.000	27	12	0.000	27	22	0.041
28	2	0.005	28	12	-0.035	28	22	-0.011
29	2	0.000	29	12	-0.002	29	22	0.027
30	2	-0.002	30	12	0.000	30	22	0.002
1	3	-0.552	1	13	0.012	1	23	0.000
2	3	0.000	2	13	-0.117	2	23	-0.003
3	3	-3.267	3	13	0.154	3	23	0.000
4	3	-0.110	4	13	0.105	4	23	0.000
5	3	-0.054	5	13	0.373	5	23	0.001
6	3	0.010	6	13	-0.027	6	23	-0.003
7	3	-0.041	7	13	0.140	7	23	0.000
8	3	-0.011	8	13	0.042	8	23	0.005
9	3	-0.027	9	13	-0.070	9	23	0.000
10	3	0.002	10	13	0.035	10	23	-0.002
11	3	0.082	11	13	0.086	11	23	0.006
12	3	0.011	12	13	-0.002	12	23	0.019
13	3	0.154	13	13	-4.998	13	23	0.008
14	3	0.062	14	13	-0.344	14	23	-0.006
15	3	-0.054	15	13	-0.044	15	23	0.000
16	3	0.002	16	13	-0.003	16	23	-0.012
17	3	-0.016	17	13	-0.005	17	23	-0.041
18	3	-0.018	18	13	0.000	18	23	-0.117
19	3	0.005	19	13	0.000	19	23	0.057
20	3	0.002	20	13	-0.001	20	23	0.063
21	3	-0.006	21	13	0.004	21	23	0.022
22	3	0.035	22	13	-0.018	22	23	0.000
23	3	0.000	23	13	0.008	23	23	-5.033
24	3	0.003	24	13	-0.004	24	23	-0.099
25	3	0.002	25	13	-0.006	25	23	-0.257
26	3	0.000	26	13	0.000	26	23	-0.031
27	3	-0.005	27	13	0.003	27	23	0.136
28	3	0.002	28	13	0.000	28	23	0.156

29	3	0.004	29	13	0.001	29	23	0.386
30	3	0.000	30	13	0.000	30	23	0.116
1	4	-0.043	1	14	0.168	1	24	0.000
2	4	0.099	2	14	-0.057	2	24	0.000
3	4	-0.110	3	14	0.062	3	24	0.003
4	4	-8.139	4	14	0.226	4	24	-0.001
5	4	-0.118	5	14	0.271	5	24	-0.001
6	4	0.005	6	14	0.012	6	24	0.000
7	4	-0.027	7	14	-0.371	7	24	0.003
8	4	0.093	8	14	-0.026	8	24	0.000
9	4	0.349	9	14	0.260	9	24	-0.001
10	4	-0.041	10	14	0.381	10	24	0.000
11	4	0.028	11	14	-0.160	11	24	0.000
12	4	-0.006	12	14	0.057	12	24	-0.003
13	4	0.105	13	14	-0.344	13	24	-0.004
14	4	0.226	14	14	-3.586	14	24	-0.002
15	4	0.070	15	14	0.000	15	24	0.000
16	4	0.000	16	14	-0.002	16	24	0.028
17	4	-0.003	17	14	-0.004	17	24	-0.006
18	4	0.004	18	14	0.000	18	24	-0.105
19	4	-0.002	19	14	0.001	19	24	0.226
20	4	0.000	20	14	0.000	20	24	-0.070
21	4	0.000	21	14	0.000	21	24	-0.043
22	4	-0.003	22	14	-0.005	22	24	0.111
23	4	0.000	23	14	-0.006	23	24	-0.099
24	4	-0.001	24	14	-0.002	24	24	-8.137
25	4	0.001	25	14	-0.002	25	24	0.117
26	4	0.000	26	14	-0.001	26	24	0.005
27	4	0.003	27	14	-0.001	27	24	-0.027
28	4	0.000	28	14	0.002	28	24	-0.093
29	4	-0.001	29	14	-0.004	29	24	0.349
30	4	0.000	30	14	0.001	30	24	0.041
1	5	0.138	1	15	0.016	1	25	-0.001
2	5	-0.256	2	15	0.063	2	25	0.001
3	5	-0.054	3	15	-0.054	3	25	0.002
4	5	-0.118	4	15	0.070	4	25	0.001
5	5	-3.549	5	15	0.358	5	25	-0.004
6	5	-0.057	6	15	0.025	6	25	-0.001
7	5	-0.058	7	15	0.091	7	25	0.000
8	5	0.052	8	15	-0.001	8	25	0.004
9	5	-0.245	9	15	-0.281	9	25	-0.001
10	5	0.268	10	15	-0.059	10	25	-0.001
11	5	-0.112	11	15	0.015	11	25	0.001
12	5	-0.029	12	15	-0.449	12	25	0.004
13	5	0.373	13	15	-0.044	13	25	-0.006

14	5	0.271	14	15	0.000	14	25	-0.002
15	5	0.358	15	15	-8.165	15	25	-0.002
16	5	-0.001	16	15	0.000	16	25	0.112
17	5	-0.004	17	15	0.000	17	25	0.029
18	5	-0.006	18	15	-0.001	18	25	0.373
19	5	0.002	19	15	0.000	19	25	-0.271
20	5	-0.002	20	15	0.000	20	25	0.358
21	5	0.001	21	15	0.000	21	25	-0.138
22	5	0.002	22	15	0.002	22	25	-0.054
23	5	0.001	23	15	0.000	23	25	-0.257
24	5	-0.001	24	15	0.000	24	25	0.117
25	5	-0.004	25	15	-0.002	25	25	-3.548
26	5	0.001	26	15	0.001	26	25	0.057
27	5	0.000	27	15	0.000	27	25	0.058
28	5	0.004	28	15	-0.002	28	25	0.052
29	5	0.001	29	15	0.000	29	25	0.245
30	5	-0.001	30	15	0.000	30	25	0.268
1	6	-0.032	1	16	0.000	1	26	0.000
2	6	0.031	2	16	-0.006	2	26	0.003
3	6	0.010	3	16	0.002	3	26	0.000
4	6	0.005	4	16	0.000	4	26	0.000
5	6	-0.057	5	16	-0.001	5	26	0.001
6	6	-8.066	6	16	0.001	6	26	0.000
7	6	0.057	7	16	0.000	7	26	0.006
8	6	0.451	8	16	0.007	8	26	-0.002
9	6	0.154	9	16	0.001	9	26	-0.001
10	6	0.008	10	16	-0.001	10	26	0.000
11	6	-0.039	11	16	0.000	11	26	0.001
12	6	0.064	12	16	0.000	12	26	-0.007
13	6	-0.027	13	16	-0.003	13	26	0.000
14	6	0.012	14	16	-0.002	14	26	-0.001
15	6	0.025	15	16	0.000	15	26	0.001
16	6	0.001	16	16	-8.069	16	26	-0.039
17	6	-0.007	17	16	-0.339	17	26	0.064
18	6	0.000	18	16	-0.087	18	26	0.027
19	6	-0.001	19	16	-0.160	19	26	0.012
20	6	-0.001	20	16	-0.015	20	26	-0.025
21	6	0.000	21	16	-0.019	21	26	-0.032
22	6	0.000	22	16	-0.082	22	26	-0.010
23	6	-0.003	23	16	-0.012	23	26	-0.031
24	6	0.000	24	16	0.028	24	26	0.005
25	6	-0.001	25	16	0.112	25	26	0.057
26	6	0.000	26	16	-0.039	26	26	-8.067
27	6	0.006	27	16	-0.060	27	26	0.056
28	6	0.002	28	16	0.010	28	26	-0.451

29	6	-0.001	29	16	0.019	29	26	0.153
30	6	0.000	30	16	-0.026	30	26	-0.008
1	7	-0.041	1	17	0.000	1	27	-0.002
2	7	-0.137	2	17	-0.019	2	27	0.000
3	7	-0.041	3	17	-0.016	3	27	-0.005
4	7	-0.027	4	17	-0.003	4	27	0.003
5	7	-0.058	5	17	-0.004	5	27	0.000
6	7	0.057	6	17	-0.007	6	27	0.006
7	7	-5.008	7	17	0.000	7	27	0.008
8	7	0.003	8	17	0.035	8	27	-0.018
9	7	0.321	9	17	-0.002	9	27	0.006
10	7	0.072	10	17	0.000	10	27	0.002
11	7	-0.060	11	17	0.000	11	27	0.000
12	7	0.158	12	17	0.002	12	27	0.000
13	7	0.140	13	17	-0.005	13	27	0.003
14	7	-0.371	14	17	-0.004	14	27	-0.001
15	7	0.091	15	17	0.000	15	27	0.000
16	7	0.000	16	17	-0.339	16	27	-0.060
17	7	0.000	17	17	-3.269	17	27	0.158
18	7	-0.003	18	17	0.002	18	27	-0.140
19	7	-0.001	19	17	0.057	19	27	-0.372
20	7	0.000	20	17	0.449	20	27	-0.091
21	7	-0.002	21	17	0.007	21	27	-0.041
22	7	0.005	22	17	-0.011	22	27	0.041
23	7	0.000	23	17	-0.041	23	27	0.136
24	7	0.003	24	17	-0.006	24	27	-0.027
25	7	0.000	25	17	0.029	25	27	0.058
26	7	0.006	26	17	0.064	26	27	0.056
27	7	0.008	27	17	0.158	27	27	-5.008
28	7	0.018	28	17	0.011	28	27	-0.003
29	7	0.006	29	17	-0.060	29	27	0.320
30	7	-0.002	30	17	-0.072	30	27	-0.072
1	8	-0.025	1	18	-0.004	1	28	0.000
2	8	0.156	2	18	0.008	2	28	0.005
3	8	-0.011	3	18	-0.018	3	28	0.002
4	8	0.093	4	18	0.004	4	28	0.000
5	8	0.052	5	18	-0.006	5	28	0.004
6	8	0.451	6	18	0.000	6	28	0.002
7	8	0.003	7	18	-0.003	7	28	0.018
8	8	-3.269	8	18	0.000	8	28	0.016
9	8	0.056	9	18	-0.001	9	28	-0.005
10	8	-0.334	10	18	0.000	10	28	0.002
11	8	-0.010	11	18	0.003	11	28	-0.007
12	8	-0.011	12	18	0.005	12	28	-0.035
13	8	0.042	13	18	0.000	13	28	0.000

14	8	-0.026	14	18	0.000	14	28	0.002
15	8	-0.001	15	18	-0.001	15	28	-0.002
16	8	0.007	16	18	-0.087	16	28	0.010
17	8	0.035	17	18	0.002	17	28	0.011
18	8	0.000	18	18	-4.997	18	28	0.042
19	8	-0.002	19	18	0.345	19	28	0.026
20	8	-0.002	20	18	-0.044	20	28	-0.001
21	8	0.000	21	18	-0.012	21	28	0.026
22	8	0.002	22	18	0.153	22	28	-0.011
23	8	0.005	23	18	-0.117	23	28	0.156
24	8	0.000	24	18	-0.105	24	28	-0.093
25	8	0.004	25	18	0.373	25	28	0.052
26	8	-0.002	26	18	0.027	26	28	-0.451
27	8	-0.018	27	18	-0.140	27	28	-0.003
28	8	0.016	28	18	0.042	28	28	-3.270
29	8	0.005	29	18	0.070	29	28	-0.056
30	8	0.002	30	18	0.035	30	28	-0.334
1	9	0.150	1	19	0.000	1	29	0.001
2	9	-0.386	2	19	0.006	2	29	0.000
3	9	-0.027	3	19	0.005	3	29	0.004
4	9	0.349	4	19	-0.002	4	29	-0.001
5	9	-0.245	5	19	0.002	5	29	0.001
6	9	0.154	6	19	-0.001	6	29	-0.001
7	9	0.321	7	19	-0.001	7	29	0.006
8	9	0.056	8	19	-0.002	8	29	0.005
9	9	-3.574	9	19	-0.004	9	29	-0.002
10	9	0.043	10	19	-0.001	10	29	-0.002
11	9	0.019	11	19	-0.002	11	29	0.001
12	9	-0.060	12	19	-0.004	12	29	-0.002
13	9	-0.070	13	19	0.000	13	29	0.001
14	9	0.260	14	19	0.001	14	29	-0.004
15	9	-0.281	15	19	0.000	15	29	0.000
16	9	0.001	16	19	-0.160	16	29	0.019
17	9	-0.002	17	19	0.057	17	29	-0.060
18	9	-0.001	18	19	0.345	18	29	0.070
19	9	-0.004	19	19	-3.585	19	29	0.259
20	9	0.000	20	19	0.001	20	29	0.281
21	9	0.001	21	19	0.168	21	29	0.150
22	9	-0.004	22	19	-0.062	22	29	0.027
23	9	0.000	23	19	0.057	23	29	0.386
24	9	-0.001	24	19	0.226	24	29	0.349
25	9	-0.001	25	19	-0.271	25	29	0.245
26	9	-0.001	26	19	0.012	26	29	0.153
27	9	0.006	27	19	-0.372	27	29	0.320
28	9	-0.005	28	19	0.026	28	29	-0.056

29	9	-0.002	29	19	0.259	29	29	-3.574
30	9	0.002	30	19	-0.381	30	29	-0.043
1	10	-0.058	1	20	0.000	1	30	0.000
2	10	0.116	2	20	0.000	2	30	-0.002
3	10	0.002	3	20	0.002	3	30	0.000
4	10	-0.041	4	20	0.000	4	30	0.000
5	10	0.268	5	20	-0.002	5	30	-0.001
6	10	0.008	6	20	-0.001	6	30	0.000
7	10	0.072	7	20	0.000	7	30	-0.002
8	10	-0.334	8	20	-0.002	8	30	0.002
9	10	0.043	9	20	0.000	9	30	0.002
10	10	-8.166	10	20	0.000	10	30	0.000
11	10	0.026	11	20	0.000	11	30	0.001
12	10	0.072	12	20	0.000	12	30	0.000
13	10	0.035	13	20	-0.001	13	30	0.000
14	10	0.381	14	20	0.000	14	30	0.001
15	10	-0.059	15	20	0.000	15	30	0.000
16	10	-0.001	16	20	-0.015	16	30	-0.026
17	10	0.000	17	20	0.449	17	30	-0.072
18	10	0.000	18	20	-0.044	18	30	0.035
19	10	-0.001	19	20	0.001	19	30	-0.381
20	10	0.000	20	20	-8.164	20	30	-0.059
21	10	0.000	21	20	-0.016	21	30	0.057
22	10	0.000	22	20	-0.054	22	30	0.002
23	10	-0.002	23	20	0.063	23	30	0.116
24	10	0.000	24	20	-0.070	24	30	0.041
25	10	-0.001	25	20	0.358	25	30	0.268
26	10	0.000	26	20	-0.025	26	30	-0.008
27	10	0.002	27	20	-0.091	27	30	-0.072
28	10	0.002	28	20	-0.001	28	30	-0.334
29	10	-0.002	29	20	0.281	29	30	-0.043
30	10	0.000	30	20	-0.059	30	30	-8.166

Tight-binding Hamiltonian for ($[\text{Mn}_3]_2\text{-}(\text{ada})_3$) $^{2+}$

1	1	-4.692	1	11	-0.121	1	21	-0.063
2	1	0.008	2	11	-0.036	2	21	-0.030
3	1	0.009	3	11	-0.051	3	21	0.020
4	1	0.098	4	11	0.362	4	21	0.154
5	1	0.067	5	11	-0.039	5	21	0.009
6	1	0.001	6	11	0.001	6	21	0.000
7	1	-0.015	7	11	0.001	7	21	0.000
8	1	-0.002	8	11	0.000	8	21	0.001
9	1	0.003	9	11	0.001	9	21	0.000
10	1	-0.002	10	11	0.000	10	21	0.000
11	1	-0.121	11	11	-7.860	11	21	-0.008
12	1	-0.035	12	11	-0.521	12	21	-0.098
13	1	-0.004	13	11	-0.082	13	21	-0.103
14	1	-0.097	14	11	-0.259	14	21	-0.007
15	1	0.077	15	11	-0.074	15	21	0.127
16	1	-0.001	16	11	-0.001	16	21	0.001
17	1	-0.005	17	11	0.001	17	21	0.000
18	1	-0.001	18	11	0.000	18	21	0.000
19	1	0.001	19	11	-0.001	19	21	0.001
20	1	0.004	20	11	-0.001	20	21	0.000
21	1	-0.063	21	11	-0.008	21	21	-8.202
22	1	0.131	22	11	0.065	22	21	0.156
23	1	0.008	23	11	0.186	23	21	-0.016
24	1	-0.093	24	11	-0.005	24	21	-0.102
25	1	-0.438	25	11	0.257	25	21	0.082
26	1	-0.003	26	11	0.000	26	21	-0.001
27	1	-0.010	27	11	0.000	27	21	0.000
28	1	0.015	28	11	0.000	28	21	-0.001
29	1	-0.002	29	11	0.000	29	21	0.000
30	1	-0.001	30	11	-0.002	30	21	0.000
1	2	0.008	1	12	-0.035	1	22	0.131
2	2	-2.927	2	12	-0.001	2	22	-0.005
3	2	0.403	3	12	-0.022	3	22	-0.039
4	2	-0.027	4	12	-0.015	4	22	-0.248
5	2	0.337	5	12	0.021	5	22	-0.051
6	2	-0.001	6	12	-0.001	6	22	0.000
7	2	0.000	7	12	-0.001	7	22	-0.001
8	2	0.001	8	12	0.000	8	22	-0.001
9	2	0.001	9	12	-0.001	9	22	0.000
10	2	-0.001	10	12	0.000	10	22	0.001
11	2	-0.036	11	12	-0.521	11	22	0.065
12	2	-0.001	12	12	-2.930	12	22	-0.072
13	2	-0.041	13	12	-0.026	13	22	0.355

14	2	0.120	14	12	0.037	14	22	-0.005
15	2	0.092	15	12	-0.004	15	22	-0.060
16	2	0.000	16	12	0.000	16	22	0.000
17	2	0.001	17	12	-0.001	17	22	-0.001
18	2	0.002	18	12	0.000	18	22	0.000
19	2	0.000	19	12	0.000	19	22	0.000
20	2	0.001	20	12	0.000	20	22	0.001
21	2	-0.030	21	12	-0.098	21	22	0.156
22	2	-0.005	22	12	-0.072	22	22	-7.718
23	2	-0.033	23	12	0.097	23	22	-0.062
24	2	0.002	24	12	0.002	24	22	0.528
25	2	0.021	25	12	0.018	25	22	0.123
26	2	0.000	26	12	-0.001	26	22	-0.001
27	2	0.000	27	12	0.000	27	22	-0.001
28	2	0.001	28	12	0.001	28	22	0.001
29	2	0.000	29	12	0.001	29	22	0.000
30	2	0.000	30	12	0.000	30	22	0.001
1	3	0.009	1	13	-0.004	1	23	0.008
2	3	0.403	2	13	-0.041	2	23	-0.033
3	3	-8.169	3	13	0.274	3	23	0.195
4	3	0.000	4	13	-0.249	4	23	0.035
5	3	0.156	5	13	0.120	5	23	0.033
6	3	0.000	6	13	0.003	6	23	0.005
7	3	0.000	7	13	0.001	7	23	0.014
8	3	0.001	8	13	0.001	8	23	0.003
9	3	0.001	9	13	0.003	9	23	0.003
10	3	-0.001	10	13	0.007	10	23	-0.011
11	3	-0.051	11	13	-0.082	11	23	0.186
12	3	-0.022	12	13	-0.026	12	23	0.097
13	3	0.274	13	13	-3.274	13	23	0.460
14	3	0.007	14	13	0.122	14	23	0.026
15	3	-0.105	15	13	0.197	15	23	0.109
16	3	0.001	16	13	0.000	16	23	-0.001
17	3	0.001	17	13	0.000	17	23	0.013
18	3	0.000	18	13	0.003	18	23	0.000
19	3	0.000	19	13	-0.003	19	23	0.005
20	3	0.000	20	13	0.007	20	23	-0.005
21	3	0.020	21	13	-0.103	21	23	-0.016
22	3	-0.039	22	13	0.355	22	23	-0.062
23	3	0.195	23	13	0.460	23	23	-4.680
24	3	0.042	24	13	0.012	24	23	-0.006
25	3	0.249	25	13	0.151	25	23	0.126
26	3	-0.001	26	13	0.003	26	23	0.001
27	3	0.000	27	13	0.005	27	23	-0.002
28	3	0.001	28	13	-0.002	28	23	0.004

29	3	0.000	29	13	-0.003	29	23	0.001
30	3	0.000	30	13	0.003	30	23	-0.005
1	4	0.098	1	14	-0.097	1	24	-0.093
2	4	-0.027	2	14	0.120	2	24	0.002
3	4	0.000	3	14	0.007	3	24	0.042
4	4	-3.255	4	14	-0.028	4	24	0.035
5	4	0.149	5	14	0.014	5	24	-0.119
6	4	0.001	6	14	0.000	6	24	0.000
7	4	-0.003	7	14	0.001	7	24	-0.001
8	4	-0.004	8	14	-0.001	8	24	0.000
9	4	0.002	9	14	0.000	9	24	0.000
10	4	0.005	10	14	0.001	10	24	0.000
11	4	0.362	11	14	-0.259	11	24	-0.005
12	4	-0.015	12	14	0.037	12	24	0.002
13	4	-0.249	13	14	0.122	13	24	0.012
14	4	-0.028	14	14	-8.032	14	24	-0.030
15	4	0.420	15	14	0.054	15	24	0.034
16	4	0.001	16	14	-0.001	16	24	-0.001
17	4	0.000	17	14	0.000	17	24	0.001
18	4	-0.003	18	14	0.000	18	24	-0.001
19	4	-0.008	19	14	0.000	19	24	-0.001
20	4	-0.001	20	14	0.000	20	24	0.001
21	4	0.154	21	14	-0.007	21	24	-0.102
22	4	-0.248	22	14	-0.005	22	24	0.528
23	4	0.035	23	14	0.026	23	24	-0.006
24	4	0.035	24	14	-0.030	24	24	-2.961
25	4	0.217	25	14	0.061	25	24	-0.027
26	4	0.000	26	14	0.002	26	24	0.000
27	4	0.004	27	14	0.001	27	24	0.000
28	4	-0.001	28	14	0.000	28	24	0.001
29	4	0.001	29	14	0.000	29	24	-0.002
30	4	-0.007	30	14	0.000	30	24	0.000
1	5	0.067	1	15	0.077	1	25	-0.438
2	5	0.337	2	15	0.092	2	25	0.021
3	5	0.156	3	15	-0.105	3	25	0.249
4	5	0.149	4	15	0.420	4	25	0.217
5	5	-7.729	5	15	-0.064	5	25	0.235
6	5	0.000	6	15	0.000	6	25	0.003
7	5	-0.001	7	15	0.005	7	25	-0.004
8	5	-0.001	8	15	-0.001	8	25	-0.001
9	5	0.001	9	15	-0.003	9	25	0.005
10	5	0.000	10	15	-0.001	10	25	-0.002
11	5	-0.039	11	15	-0.074	11	25	0.257
12	5	0.021	12	15	-0.004	12	25	0.018
13	5	0.120	13	15	0.197	13	25	0.151

14	5	0.014	14	15	0.054	14	25	0.061
15	5	-0.064	15	15	-4.659	15	25	-0.004
16	5	-0.001	16	15	0.003	16	25	0.004
17	5	0.000	17	15	-0.016	17	25	-0.006
18	5	0.000	18	15	-0.005	18	25	0.001
19	5	-0.001	19	15	0.007	19	25	0.004
20	5	0.001	20	15	-0.001	20	25	0.003
21	5	0.009	21	15	0.127	21	25	0.082
22	5	-0.051	22	15	-0.060	22	25	0.123
23	5	0.033	23	15	0.109	23	25	0.126
24	5	-0.119	24	15	0.034	24	25	-0.027
25	5	0.235	25	15	-0.004	25	25	-3.263
26	5	0.000	26	15	0.002	26	25	0.001
27	5	0.000	27	15	-0.003	27	25	-0.006
28	5	0.001	28	15	-0.013	28	25	-0.002
29	5	0.000	29	15	0.001	29	25	0.006
30	5	-0.001	30	15	0.008	30	25	0.000
1	6	0.001	1	16	-0.001	1	26	-0.003
2	6	-0.001	2	16	0.000	2	26	0.000
3	6	0.000	3	16	0.001	3	26	-0.001
4	6	0.001	4	16	0.001	4	26	0.000
5	6	0.000	5	16	-0.001	5	26	0.000
6	6	-3.035	6	16	-0.007	6	26	0.008
7	6	0.250	7	16	0.019	7	26	0.076
8	6	0.052	8	16	0.012	8	26	-0.012
9	6	-0.266	9	16	0.001	9	26	0.007
10	6	0.235	10	16	0.025	10	26	0.041
11	6	0.001	11	16	-0.001	11	26	0.000
12	6	-0.001	12	16	0.000	12	26	-0.001
13	6	0.003	13	16	0.000	13	26	0.003
14	6	0.000	14	16	-0.001	14	26	0.002
15	6	0.000	15	16	0.003	15	26	0.002
16	6	-0.007	16	16	-3.184	16	26	-0.010
17	6	0.049	17	16	-0.070	17	26	0.014
18	6	-0.094	18	16	-0.060	18	26	-0.009
19	6	0.018	19	16	-0.158	19	26	0.026
20	6	-0.024	20	16	-0.017	20	26	-0.005
21	6	0.000	21	16	0.001	21	26	-0.001
22	6	0.000	22	16	0.000	22	26	-0.001
23	6	0.005	23	16	-0.001	23	26	0.001
24	6	0.000	24	16	-0.001	24	26	0.000
25	6	0.003	25	16	0.004	25	26	0.001
26	6	0.008	26	16	-0.010	26	26	-3.196
27	6	-0.040	27	16	-0.043	27	26	-0.134
28	6	0.051	28	16	-0.066	28	26	-0.090

29	6	-0.088	29	16	0.028	29	26	0.115
30	6	0.035	30	16	0.023	30	26	-0.009
1	7	-0.015	1	17	-0.005	1	27	-0.010
2	7	0.000	2	17	0.001	2	27	0.000
3	7	0.000	3	17	0.001	3	27	0.000
4	7	-0.003	4	17	0.000	4	27	0.004
5	7	-0.001	5	17	0.000	5	27	0.000
6	7	0.250	6	17	0.049	6	27	-0.040
7	7	-2.267	7	17	-0.012	7	27	-0.004
8	7	0.093	8	17	0.068	8	27	0.028
9	7	0.187	9	17	-0.062	9	27	-0.061
10	7	-0.208	10	17	0.038	10	27	-0.028
11	7	0.001	11	17	0.001	11	27	0.000
12	7	-0.001	12	17	-0.001	12	27	0.000
13	7	0.001	13	17	0.000	13	27	0.005
14	7	0.001	14	17	0.000	14	27	0.001
15	7	0.005	15	17	-0.016	15	27	-0.003
16	7	0.019	16	17	-0.070	16	27	-0.043
17	7	-0.012	17	17	-2.191	17	27	0.077
18	7	-0.040	18	17	0.203	18	27	0.055
19	7	0.067	19	17	-0.161	19	27	0.045
20	7	0.013	20	17	0.097	20	27	0.051
21	7	0.000	21	17	0.000	21	27	0.000
22	7	-0.001	22	17	-0.001	22	27	-0.001
23	7	0.014	23	17	0.013	23	27	-0.002
24	7	-0.001	24	17	0.001	24	27	0.000
25	7	-0.004	25	17	-0.006	25	27	-0.006
26	7	0.076	26	17	0.014	26	27	-0.134
27	7	-0.004	27	17	0.077	27	27	-2.599
28	7	0.025	28	17	-0.024	28	27	-0.189
29	7	0.055	29	17	0.019	29	27	-0.349
30	7	0.038	30	17	-0.006	30	27	0.239
1	8	-0.002	1	18	-0.001	1	28	0.015
2	8	0.001	2	18	0.002	2	28	0.001
3	8	0.001	3	18	0.000	3	28	0.001
4	8	-0.004	4	18	-0.003	4	28	-0.001
5	8	-0.001	5	18	0.000	5	28	0.001
6	8	0.052	6	18	-0.094	6	28	0.051
7	8	0.093	7	18	-0.040	7	28	0.025
8	8	-3.185	8	18	0.012	8	28	0.015
9	8	0.047	9	18	-0.037	9	28	0.017
10	8	0.127	10	18	0.018	10	28	-0.079
11	8	0.000	11	18	0.000	11	28	0.000
12	8	0.000	12	18	0.000	12	28	0.001
13	8	0.001	13	18	0.003	13	28	-0.002

14	8	-0.001	14	18	0.000	14	28	0.000
15	8	-0.001	15	18	-0.005	15	28	-0.013
16	8	0.012	16	18	-0.060	16	28	-0.066
17	8	0.068	17	18	0.203	17	28	-0.024
18	8	0.012	18	18	-2.980	18	28	0.052
19	8	0.051	19	18	0.224	19	28	0.036
20	8	-0.011	20	18	-0.319	20	28	-0.081
21	8	0.001	21	18	0.000	21	28	-0.001
22	8	-0.001	22	18	0.000	22	28	0.001
23	8	0.003	23	18	0.000	23	28	0.004
24	8	0.000	24	18	-0.001	24	28	0.001
25	8	-0.001	25	18	0.001	25	28	-0.002
26	8	-0.012	26	18	-0.009	26	28	-0.090
27	8	0.028	27	18	0.055	27	28	-0.189
28	8	0.015	28	18	0.052	28	28	-2.210
29	8	-0.005	29	18	0.082	29	28	-0.091
30	8	-0.009	30	18	-0.029	30	28	-0.095
1	9	0.003	1	19	0.001	1	29	-0.002
2	9	0.001	2	19	0.000	2	29	0.000
3	9	0.001	3	19	0.000	3	29	0.000
4	9	0.002	4	19	-0.008	4	29	0.001
5	9	0.001	5	19	-0.001	5	29	0.000
6	9	-0.266	6	19	0.018	6	29	-0.088
7	9	0.187	7	19	0.067	7	29	0.055
8	9	0.047	8	19	0.051	8	29	-0.005
9	9	-3.124	9	19	0.052	9	29	0.021
10	9	0.157	10	19	0.033	10	29	0.016
11	9	0.001	11	19	-0.001	11	29	0.000
12	9	-0.001	12	19	0.000	12	29	0.001
13	9	0.003	13	19	-0.003	13	29	-0.003
14	9	0.000	14	19	0.000	14	29	0.000
15	9	-0.003	15	19	0.007	15	29	0.001
16	9	0.001	16	19	-0.158	16	29	0.028
17	9	-0.062	17	19	-0.161	17	29	0.019
18	9	-0.037	18	19	0.224	18	29	0.082
19	9	0.052	19	19	-2.391	19	29	-0.018
20	9	-0.089	20	19	0.081	20	29	0.015
21	9	0.000	21	19	0.001	21	29	0.000
22	9	0.000	22	19	0.000	22	29	0.000
23	9	0.003	23	19	0.005	23	29	0.001
24	9	0.000	24	19	-0.001	24	29	-0.002
25	9	0.005	25	19	0.004	25	29	0.006
26	9	0.007	26	19	0.026	26	29	0.115
27	9	-0.061	27	19	0.045	27	29	-0.349
28	9	0.017	28	19	0.036	28	29	-0.091

29	9	0.021	29	19	-0.018	29	29	-2.756
30	9	0.095	30	19	0.053	30	29	0.271
1	10	-0.002	1	20	0.004	1	30	-0.001
2	10	-0.001	2	20	0.001	2	30	0.000
3	10	-0.001	3	20	0.000	3	30	0.000
4	10	0.005	4	20	-0.001	4	30	-0.007
5	10	0.000	5	20	0.001	5	30	-0.001
6	10	0.235	6	20	-0.024	6	30	0.035
7	10	-0.208	7	20	0.013	7	30	0.038
8	10	0.127	8	20	-0.011	8	30	-0.009
9	10	0.157	9	20	-0.089	9	30	0.095
10	10	-2.373	10	20	0.074	10	30	-0.050
11	10	0.000	11	20	-0.001	11	30	-0.002
12	10	0.000	12	20	0.000	12	30	0.000
13	10	0.007	13	20	0.007	13	30	0.003
14	10	0.001	14	20	0.000	14	30	0.000
15	10	-0.001	15	20	-0.001	15	30	0.008
16	10	0.025	16	20	-0.017	16	30	0.023
17	10	0.038	17	20	0.097	17	30	-0.006
18	10	0.018	18	20	-0.319	18	30	-0.029
19	10	0.033	19	20	0.081	19	30	0.053
20	10	0.074	20	20	-3.228	20	30	-0.089
21	10	0.000	21	20	0.000	21	30	0.000
22	10	0.001	22	20	0.001	22	30	0.001
23	10	-0.011	23	20	-0.005	23	30	-0.005
24	10	0.000	24	20	0.001	24	30	0.000
25	10	-0.002	25	20	0.003	25	30	0.000
26	10	0.041	26	20	-0.005	26	30	-0.009
27	10	-0.028	27	20	0.051	27	30	0.239
28	10	-0.079	28	20	-0.081	28	30	-0.095
29	10	0.016	29	20	0.015	29	30	0.271
30	10	-0.050	30	20	-0.089	30	30	-3.261